國立交通大學

應用化學系碩士班

碩 士 論 文

脯氨酸雷射捕陷結晶化於溶液中之研究

Laser Trapping Crystallization of L-proline in Solution

研 究 生：黃 重 維 (Chong-Wei Huang)

指導教授：三浦 篤志 博士 (Dr. Atsushi Miura)

中 華 民 國 一 百 年 七 月

脯氨酸雷射捕陷結晶化於溶液中之研究

Laser trapping crystallization of L-proline in solution

研 究 生：黃重維　　　　Student：Chong-Wei Huang

指導教授：三浦篤志 博士　　Advisor：Dr. Atsushi Miura

國 立 交 通 大 學
應用化學系碩士班
碩 士 論 文

A Thesis
Submitted to M. S. Program
Department of Applied Chemistry
National Chiao Tung University
in Partial Fulfillment of the Requirements
for the Degree of
Master
in

Applied Chemistry

June 2011

Hsinchu, Taiwan, Republic of China

中 華 民 國 一 百 年 七 月

Laser Trapping Crystallization of L-proline in Solution

Student：Chong-Wei Huang　　　　　Advisor：Dr. Atsushi Miura

M. S. Program, Department of Applied Chemistry
National Chiao Tung University

Abstract

Photon pressure induced well-ordered molecular assembly formation technique, which has developed in our group and named as "laser trapping crystallization", is quite unique and high potential method since its spatiotemporal controllability of crystallization. Meanwhile crystallization under laser trapping is not always successful and its mechanism has not been clarified.

In this work, we studied laser trapping crystallization of a natural amino acid L-proline to clarify its crystallization dynamics and mechanism under laser trapping condition. Laser trapping crystallization of L-proline in different solvents was examined by focusing a trapping laser to the air/solution interface. We observed obvious difference of crystallization behavior depending on the solvent.

We found that the laser trapping crystallization of proline in deuterated water (D_2O) is difficult. Meanwhile in deuterated ethanol (EtOD), we succeeded the laser trapping crystallization. Crystallization of proline in EtOD is very similar to previously reported

laser trapping crystallization of glycine. Microscopic characterization of formed crystals indicates we successfully formed proline crystal by laser trapping.

In addition to crystallization, we observed locally induced liquid-liquid phase separation of proline in EtOD prior to the crystal formation, namely dense liquid droplet formation, as well as glycine in D_2O solution. Detailed observation of droplet formation dynamics enabled us to understand droplet formation dynamics and propose its mechanism.

Observed results indicate the dense droplet formation is indispensable process for laser trapping crystallization of proline in EtOD and laser trapping assembly formation, i.e. both crystallization and droplet formation, is dominated by complex contribution of various factors such as solvent characteristics, interactions between solvent and solute or solutes, and laser-induced local environment change around focal spot.
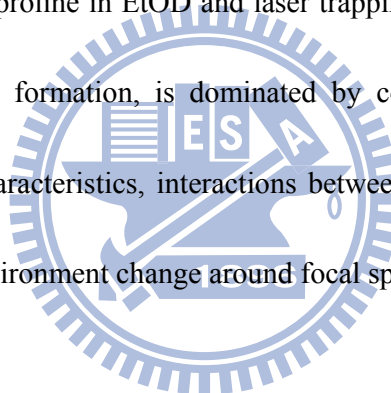
脯氨酸雷射捕陷結晶化於溶液中之研究

研 究 生：黃重維 　　　　　　　　　　指導教授：三浦篤志 博士

國立交通大學 應用化學系碩士班

中文摘要

　　雷射捕捉促使分子聚集化最近引起大家的重視，特別是它所引起更進一步的分子聚集化現象:結晶化，我們稱之為"雷射捕陷結晶化"。第一次成功示範出雷射捕陷結晶化，是在過飽和的甘氨酸重水溶液中，利用一道近紅外光的雷射聚焦在空氣與液體介面上。透過這項新穎的方法，可以達到空間及時間上控制的結晶化，還可能控制結晶的晶形結構。甚至在未飽和溶液中，光壓(雷射捕捉)可提高局部的溶液濃度至過飽和，使結晶化成功。這項新穎的結晶化被嘗試應用在許多化合物上，但並不是每一個化合物都能成功，而且它的機制尚未明瞭。

　　在這研究中，我們探討雷射捕陷結晶化動力學與其機制，基於研究與觀察脯氨酸雷射捕陷結晶化於不同的溶劑中。首先我們發現脯氨酸於重水中，雷射捕陷結晶化不易成功。藉由檢驗不一樣的溶劑至乙醇(EtOD)，我們最終成功地首次示範出脯氨酸的雷捕陷結晶化並且在結晶化前發現了其高濃度液滴的形成。高濃度液滴是一種液態/液態的相分離，藉由觀察它的形成使我們得以進一步探究在光壓下分子聚集的機制與原理。最後，根據觀察到雷射捕陷所引發的現象，我們將討論許多因素(溶劑的性質，溶質與溶劑分子的作用力與雷射引發局部溶液環境的改變)對於雷射捕陷結晶化和高密度液滴形成造成的影響，這些將助於我們對於雷射捕陷聚集化和結晶化有更深的認識。

Acknowledgement

I am very lucky and appreciate that I had chance to join this great group. Actually I stay here less than 1.5 years but the experience is so beautiful that I can not forget forever. "Global village", this word is really touched me deeply after I entering this lab. Until now, sometimes I still feel unbelievable that I work with so many foreign friends. The times here is really enjoyable and I thank everything here.

I have to appreciate to my supervisor, Prof. Miura. We have the most close and frequent contacting. Sincerely thanks to his teaching and guiding with patience and kindness, it inspired me so much that I can finish my study. I have no word to express my gratitude to him.

Thank to Prof. Masuhara. His scientific consideration and sense are stimulated and elevated to me. I am very glad and proud that I can study with him.

I also want to thank Prof. Sugiyama that he gives me lots useful suggestions. His great supporting let me clarify my research more deeply. Dr. Usman and Dr. Uwada teach me a lot and help me of experimental step up for Raman measurement. I am very grateful for their help.

Besides, I would like to thanks to all members of Masuhara group in NAIST, especially to Mr. Iino, Dr. Rungsimanon, Dr. Okano, Dr. Maezawa. They give me an impressive

memory in Japan. Additionally thanks to Dr. Yuyama, we had many discussion and that improve my understanding of my study.

I must have to thanks my seniors and classmates: 許平諭，杜靜如，李依純，劉宗翰，黃彥樺，曾繁續，許孜瑋，王順發，江威逸，黃鈴婷。Thanks for their companying with nice atmosphere and encouragement to me when I was disappointed. Specially thanks to 許平諭，杜靜如 and 劉宗翰, they help me a lot not only for daily life but also research. Thanks to 李依純, she introduced me into this group. Without her, I could not join this great group. Wish them will get great achievement in the future.

Finally, sincerely thanks to my family for their mentally and financially concerning and support to finish master degree.
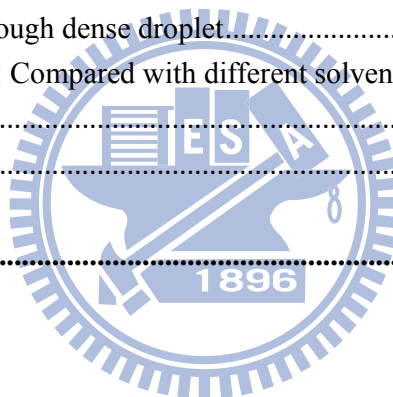
Table of Contents

List of Figures

List of Tables

1. Introduction

1.1 Laser trapping

Laser trapping has been a well-known and powerful tool for its wide application specially in biology, chemistry and physics. It can manipulate from micrometer-sized to a few tens nanometer-sized objects freely without any mechanical contact by highly focusing incident light. We have applied this technique to assemble molecules in this work.

1.1.1 History

The pioneer of laser trapping experiment, Arthur Ashkin *et al.*, found the possibility of optical trapping of transparent micron-sized particle, and finally they first demonstrated it in 1970 [1]. They reported that they could detect gradient force and scatter force when the laser beam is tightly focused on the particle.

It was not known that focused light can generate stable three-dimensional optical trap at that time. Later, Ashkin confirmed the single-beam gradient force by utilizing optical trapping method [2] and this technique has been successfully applied to the wide range of particles from dielectric to biological ones.

Chu and his colleague extended Ashkin's method to trap atoms, and he received the 1997 Nobel prize in physics along with Claude Cohen-Tannoudji and William Daniel Phillips by

the work of laser cooling and trapping of atoms [3]. Indeed it was a very big breakthrough

to control atom in the 1 Å scale. Furthermore, living cells such as bacteria can be

manipulated without damage [4].

Until nowadays, this technique has been continuously applied to the wide fields of

physical and biological studies. Usually laser trapping is applied to single micrometer-sized

particles and typically to nanoparticles, and now being developed to combine with single

molecule spectroscopy [5, 6].

1.1.2 Principle of laser trapping

Laser trapping, the physical phenomenon, is due to the interaction between light and

target objects. Traditionally, optical force is classified into two parts: gradient force and

scattering force. The former is directed along the spatial laser gradient and the latter is along

the direction of light propagation. For stable trapping of objects in three dimensional space,

the gradient force which transfers the object to the focal region must be larger to exceed the

scattering force which moves the object away from the focal region. This condition is

provided when very sharp light intensity change is achieved by using an objective lens with

high N.A.

By assuming that the object is sphere and the size is much larger than the wavelength of

trapping light, Mie scattering theory holds and the gradient force can be interpreted by Ray

optics (Fig. 1.1) [7]. Since the refraction of incident light takes place when light passed

through the object, momentum is transferred from photon to object. According to the

Newton's third law, the changed momentum of photon and that of object should be equal.

Then, if the refractive index of the trapped object is higher than that of the medium, finally

the object is moved to the focused spot as depicted in Fig. 1.2a [8]. Contrary, if the

refractive index of trapped object is lower than that of medium, the direction of optical force

is opposite as seen in Fig. 1b.
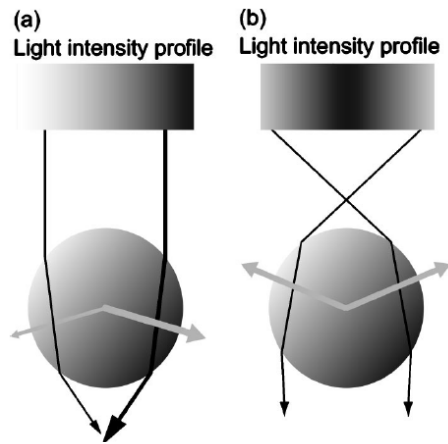
Fig. 1.1 Ray diagram shows difference of the direction of gradient force (gray arrows) induced by unfocused (a) and focused (b) light.
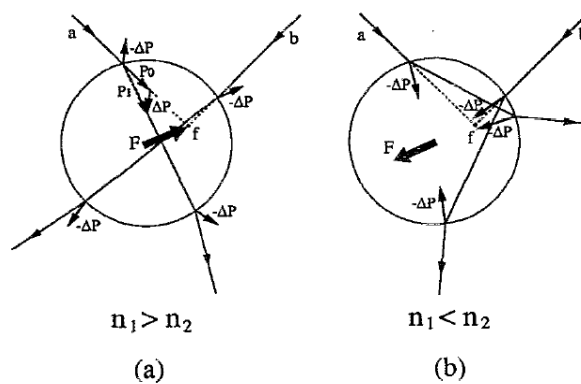
Fig. 1.2 Schematic drawing of the relationship between refractive indices of object (n_1) and medium (n_2) and the direction of gradient force.

On the other hand, Raleigh scattering is dominant in the case of trapping of small spherical object which is much smaller than the wavelength of trapping light. Under this condition the object is considered as a dielectric particle, i.e. point dipole. We need to consider the interaction between an electric field of the light and dipole moment of the particle. Gradient and scattering forces are corresponding to the first and second term of equation 1.1, respectively, where E is electric field, and B is magnetic field. An equation 1.2 depicts α which is the polarizability of a particle to be trapped, where r is the radius of the particle, and ε_2 is the dielectric constant of the surrounding medium. n_1 and n_2 are the refractive indices of the particle and the surrounding medium, respectively.

$$F = \frac{1}{2}\alpha\nabla|E|^2 + \alpha\frac{\sigma}{\sigma t}(E \times B)$$ .... (1.1)

$$\alpha = 4\pi\varepsilon_2 r^3 \frac{(n_1/n_2)^2-1}{(n_1/n_2)^2+2}$$ .... (1.2)

As the high N.A. objective lens is employed, the trapping potential becomes to the equation (1.3). Once the trapping potential overcomes the Brownian motion whose energy should be $k_B\mathrm{T}$, where k_B is the Boltzmann constant and T is the temperature in Kelvin, photon pressure makes it possible to control the object.

$$U = -\frac{1}{2}\alpha|E|^2$$ .... (1.3)

Similarly, as in Ray optics, the condition for driving the object toward the focal region,

the refractive index of the object should be larger than that of medium ($n_1 > n_2$)

1.1.3 Laser trapping-induced assembly formation

Different from single particle manipulation by laser trapping, application of this technique allowed scientists to investigate the interaction of numbers of particles such as colloids [9], polymers, and membranes [10]. Additionally, it can be applied to collect molecule. Indeed it has been demonstrated to assemble small particles of colloids and polymers [11, 12] to create their assembly which is as large as the focal spot size. Fig. 1.3 depict schematic representation of assembly formation of PNIPAM (Poly(N-isoprpryl acrylamide)) that induced by focusing of trapping light source into the solution [12]. Masuhara *et al*. have investigated the assembly formation of plenty polymer molecules under photon pressure [13-15] and its solvent dependence [16].
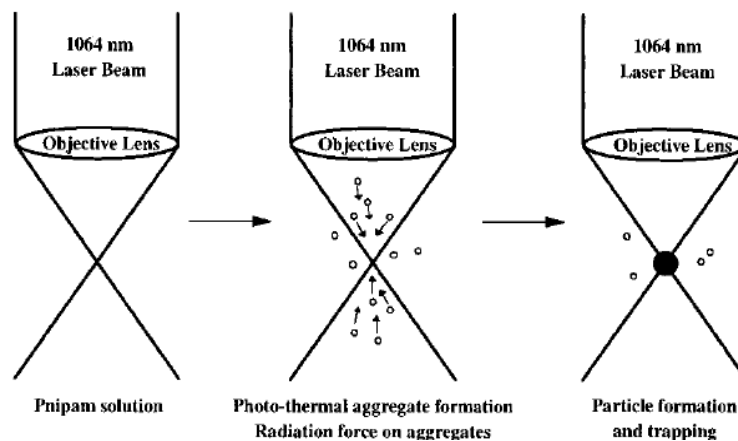
Fig. 1.3 Schematic view of PNIPAM assembly via photon pressure and phase transition [12].

On the other hand, heat generation by absorption of focused light is inevitable in laser

trapping. It induces Marangoni convection [17, 18] and enhances mass transfer [19] that

increases molecular transportation which should cooperate with photon pressure to collect

molecules. As we can see in the phase transition of PNIPAN [12], we describe this matter in

the last paragraph. Recently the convection flow under trapping could be realized in Fig. 1.4

by T. Uwada *et al.* [20].
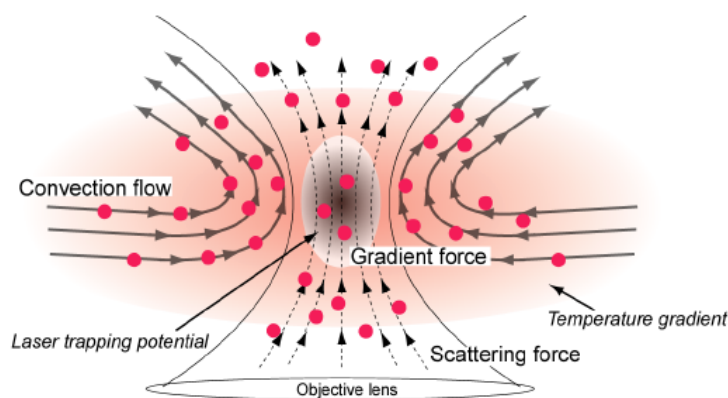
Fig. 1.4 Schematic picture of possible convection flow and trapped molecules brought up
by Uwada *et al*. [20].

Above mentioned observation of molecular assembly formations induced by laser

trapping imply a possibility of more advanced molecular assembling, i.e. well-ordered

molecular assembly such as crystallization should be possible. Tsuboi *et al*. confirmed the

assembling of several amino acids by observing their Raman scattering spectra and

backward scattering [21]. They explained that laser trapping induced assembly is probably

due to trapping clusters of solute molecules. Lysozyme was the first successful example of

laser trapping, but crystallization was observed at few days after the focused laser irradiation [22]. It reported crystallization could be induced by photon pressure causing protein aggregate. Besides, in the same proteins, lysozyme, W. Singer applied trapping to induce the crystal growth [23] and investigated directional of crystal growth under trapping [24, 25].

1.1.4 Laser trapping crystallization

Sugiyama *et al*. demonstrated glycine crystallization induced by laser trapping in 2007 [26]. It was the first observation of the crystallization only by focused irradiation. They named this method as "laser trapping crystallization". It is not only a new application of laser trapping but also novel methodology of crystallization.

In general, where and when crystallization took place is not clear, but now it is always observed at the focal spot via laser trapping within a few minutes. Moreover, they reported spatially-controlled crystal growth [27] and molecular orientation in crystal, as direction of crystal growth was directed toward laser spot and different polymorph of glycine crystal were prepared by adjusting laser power [28].

Initially, laser trapping crystallization was reported for supersaturated glycine solution. Usually it is impossible to crystallize molecules in unsaturated solution, but they can observe crystallization even in unsaturated solution by laser trapping crystallization [29]. It

suggests that local concentration increase to supersaturated value in the laser spot due to laser trapping of the clusters, leading to crystallization.

Besides, laser trapping crystallization showed not only spatiotemporally controlled crystallization but also very interesting photon pressure-induced phenomenon; large liquid droplet formation. Yuyama *et al*. demonstrated millimeter-sized dense liquid droplet formation of glycine. They observed the droplet formation by focusing the trapping laser to the solution/substrate interface [30]. Moreover, glycine crystallization was observed immediately after when the focus of trapping laser moved to the air/solution interface. It implies higher-concentration droplet formation, i.e. local concentration elevation due to the photon pressure, and they concluded that the dense droplet would be a precursor of the crystal.
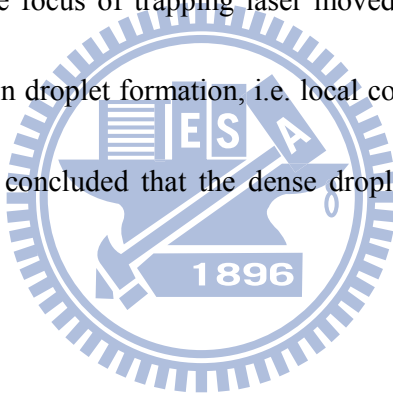
1.2 Crystallization

We study crystallization induced by laser trapping. Crystallization is closely related to our daily life such as the salt isolation from seawater and diamond formation in the deep earth under high temperature and pressure. Crystal provides molecule packing information and is used in wide fields of science and technology.

1.2.1 History and study of biomolecular crystallization

According to the history of crystallization described by McPherson [31], it can be traced back to more than 150 years ago. The first published observation of crystallization was reported by Hunefeld on hemoglobin in 1840 [32]. They reported the crystallization of blood of earthworm when it was pressed between two microscope slides. And later studies, Sumer and Stanley were awarded the Nobel Prize for chemistry in 1946 by isolation and crystallization of proteins and viruses [33]. In addition, it is also significant to analyze the structure of crystal to clarify functions of biomolecules. The first structural determination of biomolecule has done for vitamin B-12 in 1957 by D. C. Hodgkin by using its crystal [34]. She received the Novel prize for chemistry as the result of this research.

Crystallization has been studied for long time, however, its process is very complex and crystallization of some large biomolecules is still very difficult. In order to understand the fundamentals of crystallization to obtain better crystals, massive efforts were made on

optimized crystallization and crystal growth of basic molecules such as small organic

compounds and amino acids. Crystallization of amino acids, giving basic information to

understand it, is still important works for protein crystallization.

This is one of the reasons why amino acids were employed in this work. Although

crystallization is still quite empirical, further understanding of crystallization can be

expected.

1.2.2 Crystallization theory

Crystallization is a phase-transition phenomenon and also widely used as a purification

method. Usually, solution for crystallization must be under supersaturation, and for

achieving supersaturated solution there are many variable methods such as vapor pressure,

temperature and pH valve. Crystallization process can generally be separated into two parts

of nucleation and crystal growth processes. The birth of a new crystal is called nucleation: it

indicates that molecule aggregate becomes larger than the critical size. Traditionally, the

classical nucleation theory has been employed for the nucleation process, but it starts with

tiny size and it is difficult to observe experimentally (Fig. 1.5) [35]. Many papers have

studies the nucleation and its mechanism in detail [36, 37]. After nucleation, a subsequent

process is known as crystal growth where nuclei grow larger. Molecules are continuously

packing with each other in the regular ordering.
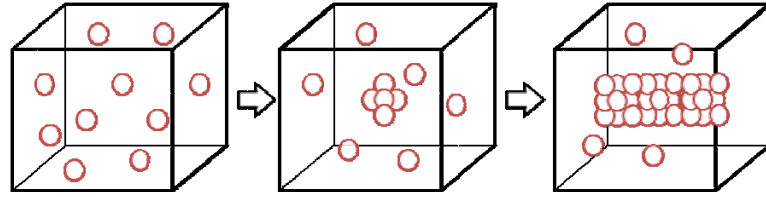
Fig. 1.5 Schematic drawing of nucleation, molecules start to pack with each other.

The process of crystallization also can be schematically illustrated by phase diagram (Fig. 1.6). The diagram is well interpreted with influential parameters of crystallization such as concentration and temperature. Under this condition, solution would be divided into three parts depending on the solution saturation. Once solution became highly saturated with higher free energy in the labile or metastable region, nucleation could take place, causing a reduction of free energy and the phase returned to the stable region. As previously mentioned, we can suppose the dense liquid is regarded as precursor of crystallization in the intermediate state as seen in Fig. 1.7 [34].
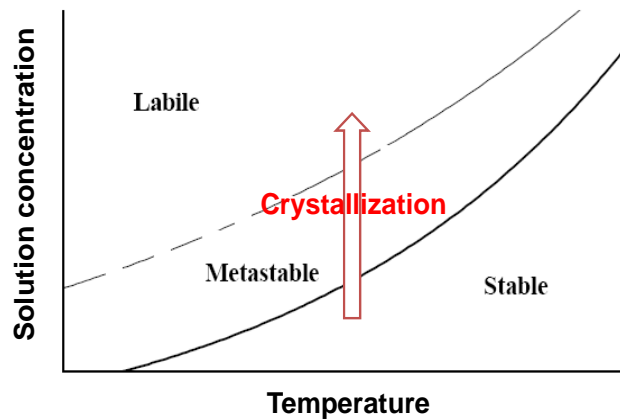
Fig. 1.6 Phase diagram showing the solubility depends on temperature and concentration.
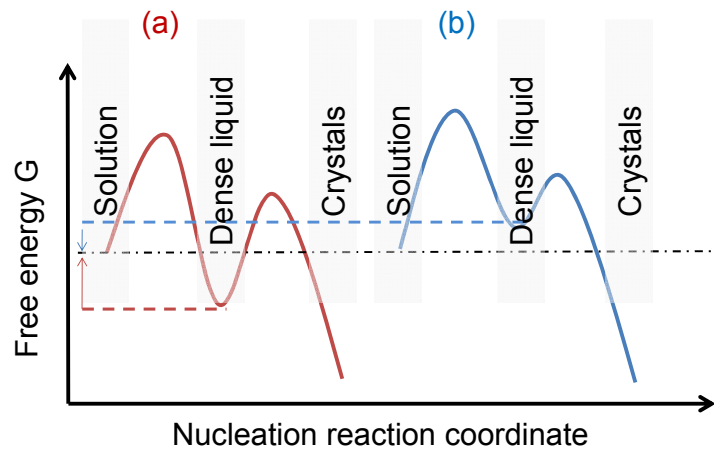
Fig. 1.7 Free energy diagram for possible crystallization processes. Curved depict phase transition from liquid, dense liquid as intermediate state, and crystalline phases. Black broken line indicates the free energy for liquid-liquid phase separation. Red and blue broken lines indicate the energy of droplet with (a) lower and (b) higher free energy than that of initial liquid phase.

1.2.3 Laser-induced crystallization

Laser has been developed since 1960. It provides very stable monochromatic light and has been applied to wide fields of chemistry, physics, biology, materials science. There are plenty of researches using lasers. Crystallization is not the exception.

There are conventional methods to crystallize such as Batch crystallization and vapor diffusion. Laser-induced crystallization has been received attention and developed because it could regularly generate crystals or control the initial orientation giving different morphology of crystals, even finding novel crystal structure. Moreover, in this work, spatiotemporally controlled control crystallization could be achieved by laser trapping. Following is the introduction of laser induced crystallization.

1.2.3.1 Photochemical reaction induced crystallization

In general, laser induced crystallization can be divided into two parts, photochemically and optically induced crystallization. The early work of the former part, John Tyndall has studied in a range of vapors and solutions in 1869 [38]. Instead of laser just irradiation with conventional lamps also could achieve photochemical crystallization [39]. In this method of crystallization, the light with high energy is enough to cause ionization or create radicals and subsequent reactions induce nucleation.

1.2.3.2 Optical crystallization

For the latter one, optically induced nucleation was discovered first by Garetz *et al*. in 1996 [40]. In their work, supersaturated solution of urea was irradiated by 20 ns pulse of 1064 nm laser light with energy of about 0.1 J per pulse. It is considered as nonphotochemical reaction because the power and wavelength of light were not able to cause photochemical reaction.

The result showed polarization dependent orientation of crystallite of urea where molecules were oriented along the incident light polarization. Authors suggested that this phenomenon was probably caused by the optical Kerr effect. Besides, following their discovery, most notably case, α- and γ- polymorphs of glycine crystals were induced from solution by circular and linear polarization of light, respectively; it is mentioned as

polarization switching [41]. Polarization switching could be made possible by the matching between packing arrangements of molecule and polarization of light. For example, α-glycine is composed of cyclic dimmers. Meanwhile γ-glycine is composed of helical chains. Recently, polarization switching was also reported in case of L-histidine [42].

Instead of Kerr effect mechanism, other nonphotochemical laser-induced crystallization method had been also developed. For example, femtosecond laser induced crystallization through bubble formation [43], single pulse crystallization via mechanism for the effect involves the isotropic electronic polarization of cluster [44] and specially this work, laser trapping crystallization.

1.3 Motivation

We are interested in molecule assembly formation and crystallization induced by photon pressure. Since for only laser trapping crystallization just succeeded in limited number of molecules and its behavior is not totally clarified, more extension of experiments involving other amino acids have been tried until now. Indeed the spatiotemporal control of crystallization through laser trapping crystallization is quite important technique. We need to understand dynamics and mechanism of molecular crystallization under photon pressure to establish this method as a general crystallization technique.

In this work, we intend to investigate the influence of different solvents so that solutions of L-proline in D_2O and EtOD were applied as sample. This would be the indication in the solvent selection. The interaction of solute with solvent affects molecule assembling under photon pressure, which was discussed base on our observation. It may imply what kind environment is efficient to allow molecules trapped, then to crystallize them, and more favorably to get their nice crystals.

Not only developing this technology but also investigating crystallization process could be extended more. As the precursor of crystallization, dense liquid induced by irradiation can also be demonstrated. We hope more understanding and extension of laser tapping crystallization can be achieved through this work.

1.4 References

1.   A. Ashkin, *Acceleration and Trapping of Patricles by Radiation Pressure.* Physical Review Letters, 1970. **24**: p. 156-159.

2.   A. Ashkin., J.M. Dziedzic, J.E. Bjorkholm, and S. Chu, *Observation of a single-beam gradient force optical trap for dielectric particles.* Optics Letters, 1986. **11**: p. 314-317.

3.   S. Chu, J.E. Bjorkholm, A. Ashkin, and A. Cable, *Experimental Observation of Optically Trapped Atoms.* Physical Review Letters, 1986. **57**: p. 314-317.

4.   A. Ashkin, J.M. Dziedzic, and T. Yamane, *Optical trapping and manipulation of single cells using infrared laser beams.* Nature, 1987. **330**: p. 314-317.

5.   M.J. Lang, P.M. Fordyce, and S.M. Block, *Combined optical trapping and single-molecule fluorescence.* Journal of Biology, 2003. **2**: p. 6.1-6.4.

6.   M.A.v. Dijk, L.C. Kapitein, J.v. Mameren, C.F. Schmidt, and E.J.G. Peterman, *Combining Optical Trapping and Single-Molecule Fluorescence Spectroscopy Enhanced Photobleaching of Fluorophores.* J. Phys. Chem. B, 2004. **108**: p. 6479-6484.

7.   K.C. Neuman and S.M. Block, *Optical trapping.* Review of Scientific Instruments, 2004. **75**: p. 2787-2809.

8.   K. Sasaki, M. Koshioka, H. Misawa, N. Kitamura, and H. Masuhara, *Optical trapping of a metal article and a water droplet by a scanning laser beam.* Appl. Phys. Lett., 1991. **60**: p. 807-809.

9.   J.C. Crocker and D.G. Grier, *When Like Charges Attract: The Effects of Geometrical Confinement on Long-Range Colloidal Interactions.* Physical Review Letters, 1996. **77**: p. 1897-1900.

10. R. Bar-Ziv and E. Moses, *Instability and "Pearling" States Produced in Tubular Membranes by Competition of Curvature and Tension.* Physical Review Letters, 1994. **73**: p. 1392-1395.

11. S.C, Chapin, V. Germain, and E.R. Dufresne, *Automated trapping, assembly, and sorting with holographic optical tweezers.* Optics Express, 2006. **14**: p. 13095-13110.

12. J. Hofkens, J. Hotta, K. Sasaki, H. Masuhara, and K. Iwai§, *Molecular Assembling by the Radiation Pressure of a Focused Laser Beam: Poly(N-isopropylacrylamide) in Aqueous Solution.* Langmuir, 1997. **13**: p. 414-419.

13. P. Borowicz, J.-i. Hotta, K. Sasaki, and H. Masuhara, *Chemical and Optical Mechanism of Microparticle Formation of Poly(N-vinylcarbazole) in N,N-Dimethylformamide by Photon Pressure of a Focused Near-Infrared Laser*

Beam. J. Phys. Chem. B, 1998. **102**: p. 1896-1901.

14. J.-i. Hotta, K. Sasaki, and H. Masuhara, *Laser-Controlled Assembling of Repulsive Unimolecular Micelles in Aqueous Solution.* J. Phys. Chem. B, 1998. **102**: p. 7687-7690.

15. T.A. Smith, J.-i. Hotta, K. Sasaki, H. Masuhara, and Y. Itoh|, *Photon Pressure-Induced Association of Nanometer-Sized Polymer Chains in Solution.* J. Phys. Chem. B, 1999. **103**: p. 1160-1163.

16. P. Borowicz, J.-i. Hotta, K. Sasaki, and H. Masuhara, *Laser-Controlled Association of Poly(N-vinylcarbazole) in Organic Solvents: Radiation Pressure Effect of a Focused Near-Infrared Laser Beam.* J. Phys. Chem. B, 1997. **101**: p. 5900-5904.

17. M. Gugliotti, M.S. Baptista, and M.J. Politi, *Laser-Induced Marangoni Convection in the Presence of Surfactant Monolayers.* Langmuir, 2002. **18**: p. 9792-9798.

18. Z.-S. MaoI and J. Chen, *Numerical simulation of the Marangoni effect on mass transfer to single slowly moving drops in the liquid-liquid system.* Chemical Engineering Science, 2004. **59**: p. 1815-1828.

19. O.A. Louchev, S. Juodkazis, N. Murazawa, S. Wada, and H. Misawa, *Coupled laser molecular trapping,cluster assembly, and deposition fed by laser-induced Marangoni convection.* Optics Express, 2008. **16**: p. 5673-5680.

20. T. Uwada, T. Sugiyama, A. Miura, and H. Masuhara, *Wide-field light scattering imaging of laser trapping dynamics of single gold nanoparticles in solution.* Proc. of SPIE, 2010. **7762**: p. 77620N-1~8.

21. Y. Tsuboi, T. Shoji, and N. Kitamura, *Optical Trapping of Amino Acids in Aqueous Solutions.* J. Phys. Chem. C, 2010. **114**: p. 5589-5593.

22. Y. Tsuboi, T. Shoji, and N. Kitamura, *Crystallization of Lysozyme Based on Molecular Assembling by Photon Pressure.* Japanese Journal of Applied Physics, 2007. **114**: p. L1234-L1236.

23. W. Singer, U.J. Gibson, T.A. Nieminen, N.R. Heckenberg, and H. Rubinsztein-Dunlop, *Towards Crystallization using Optical Tweezers.* Proc. of SPIE, 2006. **6038**: p. 60380B-1~8.

24. W. Singer, T.A. Nieminen, U.J. Gibson, N.R. Heckenberg, and H. Rubinsztein-Dunlop, *Orientation of optically trapped nonspherical birefringent particles.* Physical Review 2006. **73**: p. 1-5.

25. W. Singer, H. Rubinsztein-Dunlop, and U. Gibson, *Manipulation and growth of birefringent protein crystals in optical tweezers.* Optics Express, 2004. **12**: p. 6440-6445.

26. T. Sugiyama, T. Adachi, and H. Masuhara⌐, *Crystallization of Glycine by Photon Pressure of a Focused CW Laser Beam.* Chemistry Letters, 2007. **36**: p. 1480-1481.

27. T. Sugiyama, T. Adachi, and H. Masuhara, *Crystal Growth of Glycine Controlled by a Focused CW Near-infrared Laser Beam.* Chemistry Letters, 2009. **38**: p. 482-483.

28. T.Rungsimanon, K.-i. Yuyama, T. Sugiyama, H. Masuhara, N. Tohnai, and M. Miyata, *Control of Crystal Polymorph of Glycine by Photon Pressure of a Focused Continuous Wave Near-Infrared Laser Beam.* J. Phys. Chem. Lett., 2010. **1**: p. 599-603.

29. T. Rungsimanon, K.-i. Yuyama, T. Sugiyama, and H. Masuhara, *Crystallization in Unsaturated Glycine/D₂O Solution Achieved by Irradiating a Focused Continuous Wave Near Infrared Laser.* Crystal Growth & Design, 2010. **10**: p. 4686-4688.

30. K.-i. Yuyama, T. Sugiyama, and H. Masuhara, *Millimeter-Scale Dense Liquid Droplet Formation and Crystallization in Glycine Solution Induced by Photon Pressure.* J. Phys. Chem. Lett., 2010. **38**: p. 1321-1325.

31. A. McPherson, *Crystallization of biological macromolecules.* 1999, New York, USA Cold Spring Harbor Laboratory Press.

32. F.L. Hünefeld, Der Chemismus in der thierischen Organisation, 1840: p. 158-163.

33. W.M. Stanley, *Isolation of a crystalline protein possessing the properties of tobacco-mosaic virus.* Science, 1935. **81**: p. 644-645.

34. D.C. Hodgkin, J. Kamper, J. Lindsay, M. MacKay, J. Pickworth, J.H. Robertson, C.B. Shoemaker, J.G. White, R.J. Prosen, and K.N. Trueblood, *The Structure of Vitamin B12 I. An Outline of the Crystallographic Investigation of Vitamin B12.* Proc. R. Soc. Lond. A, 1957. **242**: p. 228-263.

35. P.G. Vekilov, *Dense Liquid Precursor for the Nucleation of Ordered Solid Phases from Solution.* Crystal Growth & Design, 2004. **4**: p. 671-685.

36. J.M. Garcı´a-Ruiz, *Nucleation of protein crystals.* Journal of Structural Biology, 2003. **142**: p. 22-31.

37. A.A. Chernov, *Protein crystals and their growth.* Journal of Structural Biology, 2003. **142**: p. 3-21.

38. J. Tyndall, Philos. Mag. , 1869. **37**: p. 384.

39. S.p. Veesler, K. Furuta, H. Horiuchi, H. Hiratsuka, N. Ferte, and T. Okutsu, *Crystals from Light Photochemically Induced Nucleation of Hen Egg-White Lysozyme.* Crystal Growth & Design, 2006. **6**: p. 1631-1635.

40. B.A. Garetz, N. J. E. Aber, L. Goddard, R.G. Young, and A.S. Myerson, *Nonphotochemical, Polarization-Dependent, Laser-Induced Nucleation in Supersaturated Aqueous Urea Solutions.* Physical Review Letters, 1996. **77**: p. 3475-3476.

41. B.A. Garetz and J. Matic, *Polarization Switching of Crystal Structure in the Nonphotochemical Light-Induced Nucleation of Supersaturated Aqueous Glycine Solutions.* Physical Review Letters, 2002. **89**: p. 177501-1~4.

42.   X. Sun, B.A. Garetz, and A.S. Myerson, *Polarization Switching of Crystal Structure in the Nonphotochemical Laser-Induced Nucleation of Supersaturated Aqueous L-Histidine.* Crystal Growth & Design, 2008. **8**: p. 1720-1722.

43.   K. Nakamura, Y. Sora, H.Y. Yoshikawa, Y. Hosokawa, R. Murai, H. Adachi, Y. Mori, T. Sasaki, and H. Masuhara, *Femtosecond laser-induced crystallization of protein in gel medium.* Applied Surface Science, 2007. **253**: p. 6425-6429.

44.   A.J. Alexander and P.J. Camp, *Single Pulse, Single Crystal Laser-Induced Nucleation of Potassium Chloride.* Crystal Growth & Design, 2009. **9**: p. 958-963.
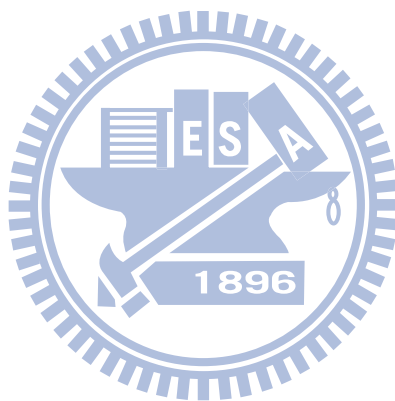
2. Experimental

2.1 Materials

D$_2$O (>99%), EtOD (>99%), and L-proline (>99%) were obtained from Sigma-Aldrich

and used without any further purification. Concentration of D$_2$O and EtOD solution of

L-proline is ranging 1.500 ~ 1.950 g/mL and 0.006 ~ 0.020 g/mL, respectively. Solute

molecules in the solution were ensured to be totally dissolved by heating with a water bath

to 60°C for 8-12 h in the glass vial (Nichiden-Rika glass) and then the solution was left until

it returned to room temperature (~25°C). Prior to the laser trapping crystallization

experiments solutions were aged for 1 to 7 days to ensure the absence of spontaneous

crystallization. Here we used deuterated water and ethanol (D$_2$O and EtOD, respectively) as

solvents to suppress temperature elevation due to trapping laser absorption. Details are

discussed in section 2.5.

Since an experimental requirement to focus trapping laser light to the solution surface

with a short-working distance objective lens, two different types of sample containers were

mainly used in this study. First is a flat glass substrate. A cover glass (24 mm × 30 mm,

Gold Seal) was mainly employed for EtOD solution of L-proline (Fig. 2-1a). In contrast,

D$_2$O solution of L-proline is highly viscous and difficult to be spread forming thin layer of

the solution on the cover glass. Thus trapping laser cannot reach to the solution surface. To

achieve thinner thickness of proline/D_2O solution, a bottom glass dish (Ibidi, μ-dish, 35mm

high and 2 cm diameter) was mainly used (Fig. 2-1b) as the second sample container. For

additional experiments in section 6.2, we use a home-made closed glass container which

was fabricated by cutting glass vial (Nichiden-Rika glass) and glued on a cover slip by

silicon glue (Shin-Etsu Silicone, 1 component RTV).

A shape of solution surface depends on what sample container is used. The surface shape

of flat cover glass slip was convex and other two (bottom glass dish and cut glass vial

container) were concave. Shapes and a distribution of solution thickness on different

containers were depicted Fig. 2.1. Solution height distribution of cut glass vial container is

similar to that of bottom glass dish. Applied volume of the solution was changed to adjust

an initial solution thickness at the center to be about 70~150 μm for all conditions.

Before usage of the containers, all containers were washed with detergent, acetone and

purified water repeatedly. Washed containers were further cleaned by dry washing method

with applying oxygen plasma treatment (10 minutes with oxygen gas flow rate of 40

cc/min). After wet and dry cleanings surface of all glass containers became highly

hydrophilic and clean. Applied solution to clean and hydrophilic surface spreads and covers

whole glass surface stably.

(a) Cover glass
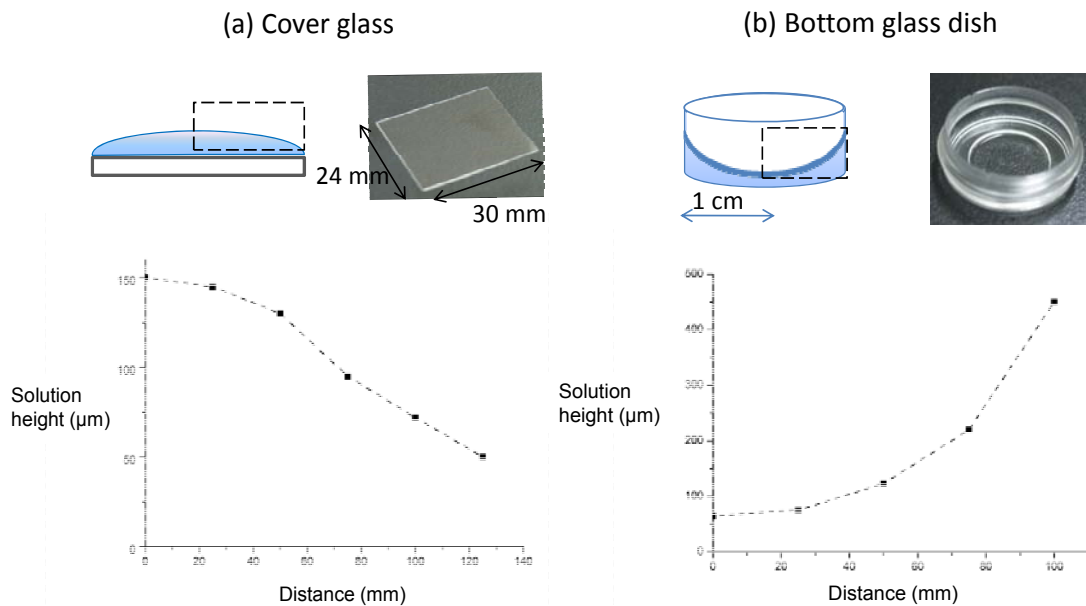
(b) Bottom glass dish

Fig. 2.1 Solution height distribution in (a) cover glass and (b) bottom glass dish

2.2 Microscope set up: Imaging and spectroscopy

Fig. 2.2 schematically shows a microscope setup used in time-resolved laser trapping crystallization imaging and dynamics study. Microscope setup is based on an inverted microscope (Olympus, IX71). Room temperature and humidity were controlled to be around 23~25°C and 50~60%, respectively. Linearly polarized near-infrared continuous wave 1064 nm Nd:YVO$_4$ laser (Coherent, Matrix CW) was employed as a trapping light source. The trapping laser was introduced into the microscope and focused to the air/solution interface through a 40× objective lens (N.A. 0.95). In order to achieve optimal trapping condition, trapping laser light was expanded and collimated to fully use pupil diameter of a microscope objective lens (~8 mm).

The other laser, 488 nm CW diode laser (Spectra-Physics, model name, 20 mW) was also

introduced into the microscope coaxially with a trapping NIR laser to check solution surface

and a focusing position of NIR laser. It was also used as a scattering light source in the

backward scattering measurement by collecting its reflection light with EMCCD camera.

Crystallization behavior near the laser spot was monitored and recorded by CCD or

EMCCD camera. Bright field transmission imaging has carried out by using a halogen lamp

as an illumination light source. Sample solutions were covered to suppress quick

evaporation of solution during the measurement.
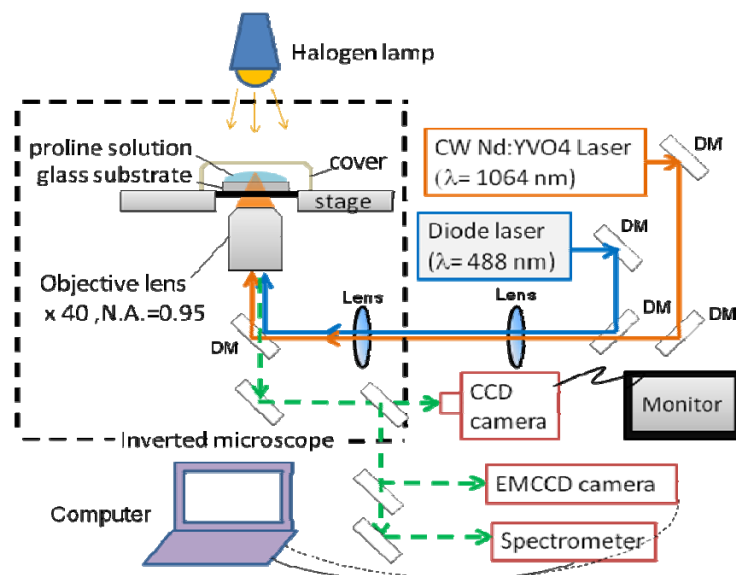
Fig. 2.2 Schematic diagram of optical set up of laser trapping crystallization system.

Confocal Raman scattering measurement was performed to characterize obtained crystals

with an inverted microscope-based laser scanning confocal microscope (Olympus, FV300),

where schematic diagram of confocal Raman system is shown in Fig. 2.3. A 532 nm DPSS

laser (40 mW, JLW-532-200, SLOC) was employed as probe laser with the power ranger of

30-40 mW.
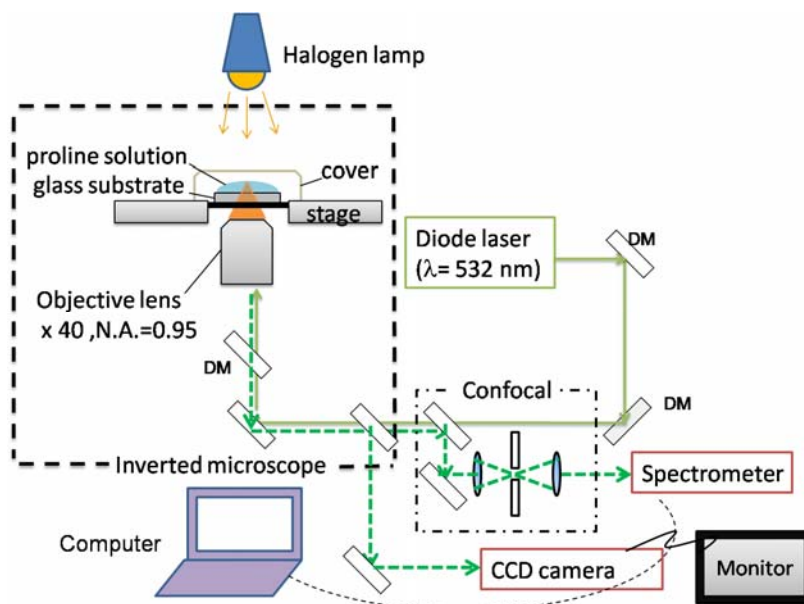
Fig. 2.3 Schematic diagram of optical set up of laser scanning confocal microscope.

Raman scattering signals were detected by cooled CCD camera (PIXIS400, Princeton instruments) combined with polychromator with a 150 grooves/mm grating (SpectraPro 2300i, Princeton instruments) through filter (Single-notch filter). We employed same objective lens (40×. N.A. 0.95) lens for Raman scattering measurement under laser trapping crystallization. All spectra were measured by integrating the signal for ~10 min. Proline crystals obtained by laser trapping crystallization in EtOD were buried in a transparent superglue to prevent a deliquescence by exposing to the water in the air.

2.3 Characteristics of proline

Proline is one of the twenty proteinogenic amino acids. It is unique in amino acids. It has pyrrolidine ring as main framework and α-amino group in its ring is secondary. Chemical structure of proline is depicted in Fig. 2.4 Proline can alternate its form from uncharged to the zwitterionic [1, 2]. Energetic difference of these two forms is negligibly small and structural transformation can occur smoothly.
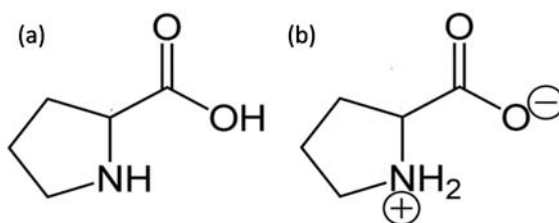
Fig. 2.4 Chemical structure of proline. (a) Neutral and (b) zwitterionic form

The heterocyclic ring gives exceptional rigidity compared to the other amino acids despite its flexibility. Characteristic ring structure gives directionality in biological systems despite its conformational flexibility. Thus, proline is often found at the end of helix or in turns or loops in protein structure. Conformational flexibility of proline draws much attention since it is important for chemical reactivity and biological functionality for many molecules [1].

Proline is well-known as a highly hygroscopic compound. It suggests that proline strongly interacts with water molecule. It will break the intermolecular hydrogen bond between prolines easily [3] that confirmed from the Raman scattering spectra. Suppression

of vibronic motions of carboxyl group on the proline molecule is interpreted due to the coordination of water molecule. It implies strong interactions between proline and water molecule [3-5]. According to its high affinity with water molecule, proline shows very high solubility in water (~1.6 g/mL, 23°C). Actually, addition of proline to some proteins can increase the solubility [5]. Solubility of proline in different solvent [6, 7] applied in this study are is listed in table 2.1 with refractive indices and boiling points.

Table 2-1 Property of D_2O and EtOD, and solubility of L-proline of them

	D_2O	EtOD
Solubility of proline	1.9 g/ml (23°C)	0.012 g/ml (19 °C, EtOH)
Refractive index	1.33 (H_2O)	1.36 (EtOH)
Boil point	100°C	79°C

The crystal structure of L-proline was first reported by Barbara *et al.* in 1949 [8]. Based on the hygroscopic character, it is difficult to form and grow water-free crystals and deterioration of crystals due to brief exposure to the atmospheric water vapor is not avoidable. The unit cell of the crystal was found to be orthorhombic with space group of $P2_12_12_1$ and L-proline molecules were connected by intermolecular hydrogen-bonding as shown in Fig. 2.5 [9]. Fig. 2.6 shows proposed molecular arrangement with taking into account of hydrogen bonding between water and proline based on crystal structure [5].
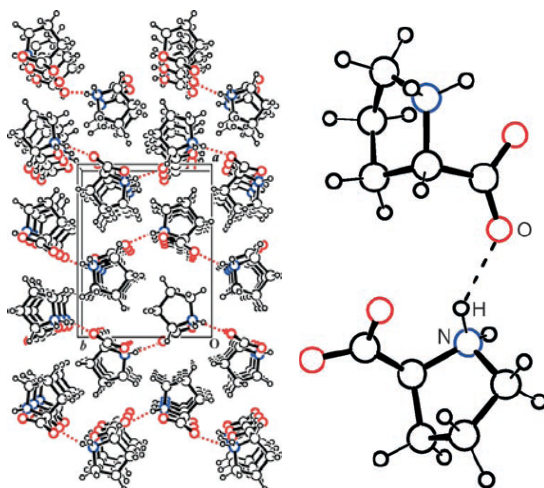
Fig. 2.5 (a) Crystal structure of L-proline and (b) hydrogen-bonded dimer structure formed between the columns in a crystal.
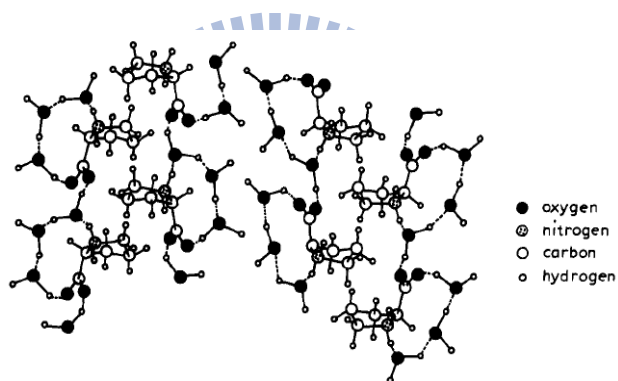
Fig. 2.6 Proposed model of the molecular arrangement of L-proline and water in a saturated proline solution.

2.4 Estimation of local temperature elevation induced by trapping laser irradiation

Under laser trapping condition, temperature elevation due to laser absorption cannot be avoided. We should consider it since temperature change affects physical property and chemical reactivity of molecules in the solution. In general, temperature elevation causes increasing solubility of solute molecule and decreasing supersaturated value (SS). However,

temperature elevation enhanced evaporation of solvent and increasing of supersaturated value can occur simultaneously. Thus we need to estimate temperature elevation due to the absorption of trapping laser light at 1064 nm quantitatively.

Investigations of temperature increasing under laser trapping condition have been reported. In the case of 1064 nm CW YAG laser, Fischer reported that $\Delta T/\Delta P \sim 5$ K/W by thermal handing of langmuir-monolayers at the air/water interface [10]. Here T and P represent temperature in Kelvin and irradiated laser power in Watt. Schmid and Tromberg reported ~ 8 K/W and 10-14.5 K/W of temperature elevation of water, respectively [11-12]. Ito reported solvent dependent temperature elevation degree difference for ethylene, ethanol, and water as $\sim 62\pm 6$, 49 ± 7, and 23 ± 1 K/W in ethylene, ethanol, and water, respectively, in small domain of solution base on the diffusion coefficient of fluorescent molecular determined by FCS [13].

Here heat is generated by irradiated laser light that was absorbed by solvent and solute molecules. First, we checked the absorption by solvent and solute molecules on the basis of Beer-Lambert's Law,

$$I = I_0 e^{-\alpha l} = I_0 10^{-\varepsilon bc} \quad \text{……….……….…………} (2\text{-}1)$$

where I_0 and I are the intensity of incident and transmitted light, respectively. α and l are absorption coefficient and optical path length. Absorption also can be defined based on molar absorption coefficient ε, optical length b, and concentration c.

28

Fig. 2.7 shows the optical path length dependent transmittance change of H_2O, D_2O, EtOH, EtOD, and L-proline aqueous solution measured at 1064 nm. All the absorption and transmittance spectra were measured by absorption spectrophotometer (JASCO, V-600). As depicted in Fig. 2.7 optical path length dependent exponential decrease of transmittance was observed for all samples. Deuterated solvents showed smaller diminution of transmittance than that of H_2O and EtOH. It indicates that deuterated solvents absorb less 1064 nm light and, as a result, temperature elevation is smaller than others. Therefore we decided to use deuterated solvent to prevent temperature elevation in this research. By fitting the exponential curve based on the least square method, absorption coefficients of each solvent are as follows; H_2O is ~ 14.5 m^{-1}, D_2O is ~1 m^{-1}, and EtOH is ~11 m^{-1}, and EtOD is ~4.6 m^{-1}.

A contribution of L-proline molecule in an absorption of L-proline solution can be obtained from eq. 2-2, where x and y in the equation indicate solvent and proline respectively.

$$e^{-\alpha \times l} = 10^{-(\varepsilon_x b_x c_x + \varepsilon_y b_y c_y)}$$ …………………………. (2-2)

Molar absorption coefficient of proline at 1064 nm is obtained as ~ 5.0×10^{-3} $M^{-1}cm^{-1}$ from a mixture of 1.93M L-proline and 46.29 M water solution (Eq. 2-3). Compared to water, it is about five times larger than that of water (1.1×10^{-3} $M^{-1}cm^{-1}$).

$$e^{-14.28 \times 0.01} = 10^{-(1.13 \times 10^{-3} \times 1.0 \times 46.29 + \varepsilon_{pro} \times 1.0 \times 1.93)} \quad \dots\dots\dots\dots (2\text{-}3)$$
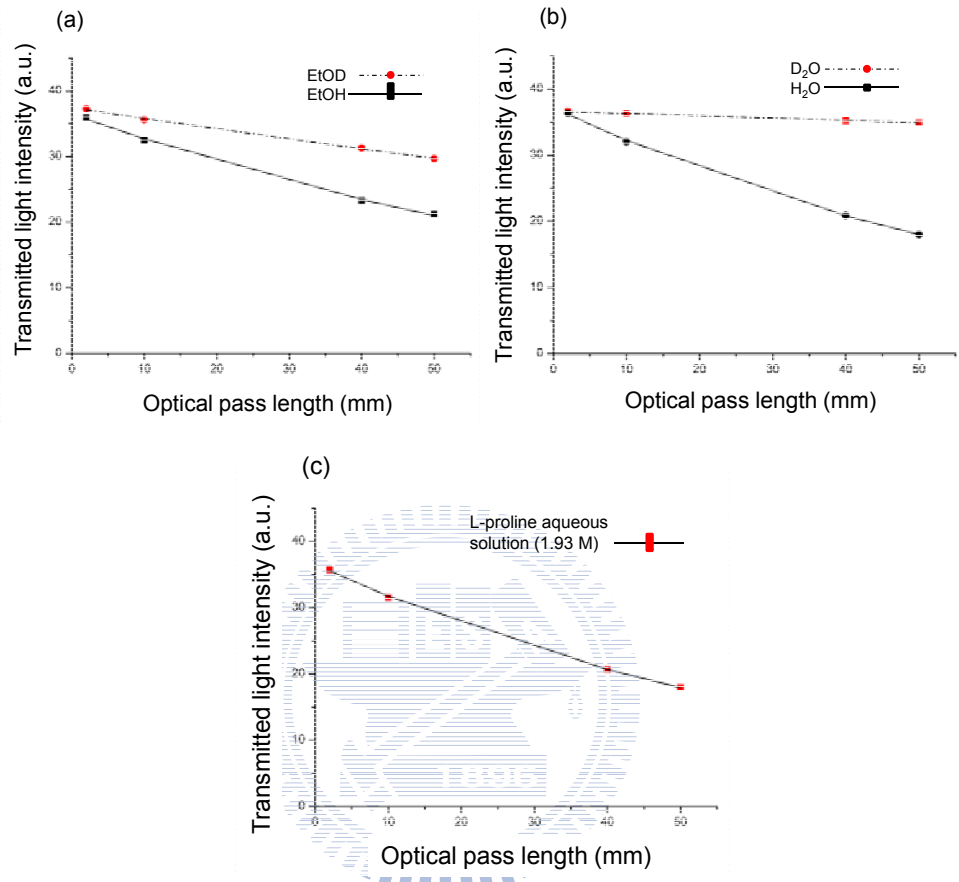
Fig. 2.7 Optical path length dependence of transmittance of (a) EtOD and EtOH, (b) D_2O and H_2O and (c) L-proline aqueous solution.

If we assume effective optical path length is represented by focal volume size dimension and we can estimate absorption by eq. 2-4 and the horizontal and lateral size of focal volume can be derived from egs. 2-5 and 2-6,

$$A_{abs} = \frac{\alpha d}{2.3} = \frac{\alpha z_0}{2.3} \quad \dots\dots\dots\dots\dots\dots\dots\dots\dots\dots (2\text{-}4)$$

$$Z_0 = 1.4 \times \lambda \times \frac{n}{NA^2} \quad \dots\dots\dots\dots\dots\dots\dots\dots\dots (2\text{-}5)$$

$$r_0 = 0.5 \, w_0 = 0.61 \times \lambda / NA \quad \ldots\ldots\ldots\ldots\ldots\ldots\ldots \text{(2-6)}$$

where r_0, Z_0, λ, NA, and n are the short and long axes, wavelength of light, numerical

aperture of the objective lens and refractive index of medium, respectively. Values of λ, NA,

and n of solvents are known. Therefore r_0 and Z_0 are estimated to be 0.68 and 2.25 μm,

respectively.

Trapping laser light is tightly focused by high NA objective lens. If we consider only a

central part contribute to the absorption and heat generation, the temperature elevation in

the focal spot is represented by equation 2-7, where T, P and κ are temperature, laser power

(W) and thermal conductivity, respectively [14].

$$\Delta \frac{T}{P} = \frac{A_{abs}}{2\sqrt{\pi}\kappa r_0} \quad \ldots\ldots\ldots\ldots\ldots\ldots\ldots\ldots\ldots\ldots\ldots\ldots\ldots \text{(2-7)}$$

Parameters in table 2-2 are substituted to eq. 2-7, and we can estimate the temperature

elevation degree during laser trapping.

Table 2-2 Absorption coefficient (1064 nm), thermal conductivity and estimation of temperature elevation by irradiation (1064 nm) in different solvent

Sample	α ,absorption coefficient (m^{-1})	κ ,thermal Conductivity [W $m^{-1}K^{-1}$]	Temperature elevation ($\triangle$T/P)
H_2O	14.5	0.59	~9.9
D_2O	0.98	0.59 (H_2O)	~0.7
EtOH	11.0	0.17	~26.0
EtOD	4.6	0.17 (EtOH)	~10.9

2.5 References

1. J. Kapitan, et al., *Proline Zwitterion Dynamics in Solution, Glass, and Crystalline State.* Journal American Chemical Society, 2006. **128**: p. 13454-13462.

2. R. Wu and T.B. McMahon, *Infrared Multiple Photon Dissociation Spectra of Proline and Glycine Proton-Bound Homodimers. Evidence for Zwitterionic Structure.* Journal American Chemical Society, 2007. **129**: p. 4864-4865.

3. P. Zhang, et al., *Neutron spectroscopic and Raman studies of interaction between water and proline.* Chemical Physics, 2008. **345**: p. 196-199.

4. M. Civera, M. Sironi, and S.L. Fornili, *Unusual properties of aqueous solutions of L-proline:A molecular dynamics study.* Chemical Physics Letters, 2005. **415**: p. 274-278.

5. B. Schobert and H. Tschesche, *Unusual solution properties of proline and its interaction with proteins.* Biochimica et Biophysica Acta, 1978. **541**: p. 270-277.

6. H.-D. Belitz, W. Grosch, and P. Schieberle, *Food Chemistry* 2009: Springer.

7. M. Jelifiska-Kazimierczuk and J. Szydlowski, *Isotope Effect on the Solubility of Amino Acids in Water.* Journal of Solution Chemistry,, 1996. **25**(12): p. 1175-1184.

8. B.A. Wright and P.A. COLE, *Preliminary examination of the crystal structure of l-proline.* Aeta Cryst., 1949. **2**: p. 129-130.

9. Y. Hayashi, et al., *Large Nonlinear Effect Observed in the Enantiomeric Excess of Proline in Solution and That in the Solid State.* Angew. Chem. Int. Ed., 2006. **45**: p. 4593-4597.

10. S. Wurlitzer, et al., *Micromanipulation of Langmuir-Monolayers with Optical Tweezers.* J. Phys. Chem. B, 2001. **105**: p. 182-187.

11. E.J.G. Peterman, F. Gittes, and C.F. Schmidt, *Laser-Induced Heating in Optical Traps.* Biophysical Journal, 2003. **84**: p. 1308-1316.

12. Liu Y., et al., *Physiological Monitoring of Optically Trapped Cells: Assessing the Effects of Confinement by 1064-nm Laser Tweezers Using Microfluorometry.* Biophysical Journal, 1996. **71**: p. 2158-2167.

13. S. Ito, et al., *Application of Fluorescence Correlation Spectroscopy to the Measurement of Local Temperature in Solutions under Optical Trapping Condition.* J. Phys. Chem. B, 2007. **111**: p. 2365-2371.

14. D. Walgraef, N.M. Ghoniem, and J. Lauzeral, *Deformation pattern in thin films under uniform laser irradiation.* Physical Review B, 1997. **15**: p. 361-376.

3. Laser Trapping Crystallization of L-proline

in Deuterated Water (D$_2$O)

Based on the experience in glycine, laser trapping crystallization has only been achieved by focusing near-infrared laser to the air/solution interface [1]. It suggests that utilization of the interface increases possibility of crystallization. Thus we follow the previous example, L-proline crystallization was examined by setting the focus at the air/solution interface. Here I used bottom glass dish to prepare thin layered sample solution.

3.1 Surface deformation, crystallization, and dry spot formation

As mentioned in the previous chapter, local heating induced by irradiation is inevitable. Induced surface temperature elevation decreases the surface tension causes local solution surface deformation and height change along the distribution of Gaussian laser beam [2-5]. As we see in Fig. 3.1a solution surface height became lower by focusing trapping laser to the surface. Lowering rate depends on applied laser power. Higher power shows faster change of the height. It can be explained by higher temperature elevation with higher power. Interestingly, the lowering rate of solution height depends on the initial solution height as shown in Fig.3.1b. If initial solution height exceeds 100 μm, it takes much longer time solution layer to be very thin. Because not only the walled container suppressed the solution

deformation, but also high viscosity of proline solution resisted the surface change.
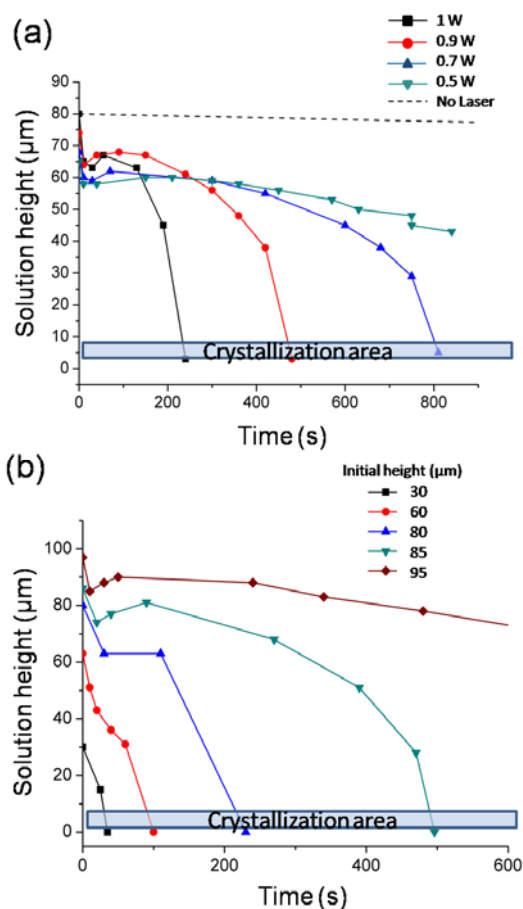
Fig. 3.1 (a) Power and (b) initial solution height dependent local solution height change. Supersaturated value was 0.9 SS. Power dependence measured with 0.5, 0.7, 0.9, 1.0 W and no laser irradiation. Lower panel shows initial solution height dependence measured with 30, 60, 80, 85 and 95 μm. Laser power was 1.0 W.

By further irradiation of trapping laser after lowering the surface height to be very thin

(1~5 μm), crystallization was frequently observed. However, the crystal shape was always

flat polycrystal and it grew quite rapidly probably due to its layer thinness and high

concentration. Actually its size can reach up to more than 100 μm within 1 sec. Fig. 3.2a

shows a bright-field image of trapping-induced crystal which was taken by CCD camera

under microscope. Whole view of the crystal in the container is depicted in Fig. 3.3a. Solution height could not be checked anymore after crystallization, but it seemed that the height is slightly recovering.
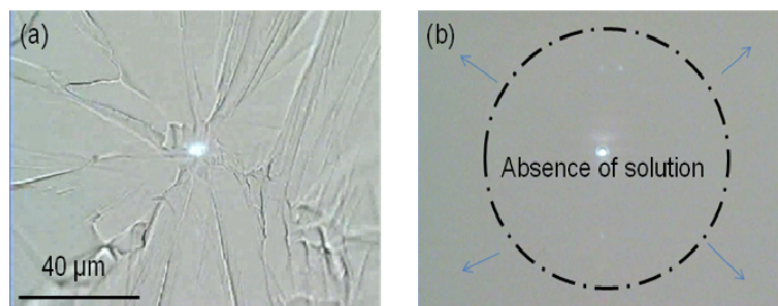
Fig. 3.2 Further irradiation, solution height was decreased to near the bottom glass substrate and then gave two results. (a) Crystallization (b) Local totally dry, absence of solution.

Similar polycrystals can be formed when the solvent was evaporated. Crystals formed by self-evaporation are shown in Fig. 3.3b. We frequently observed that crystallization started from the outside of microscope view and propagation of the growth front passed whole view.

In contrast, we sometime observed a small dry spot at the surrounding of the laser spot as seen in Fig. 3.2b. No crystallization was observed in this case. Drying indicates absence of both solvent and solute molecules around the laser spot. It should be noted that observed dry spot formation is quite local phenomena occurring only near the focused laser spot, and surprisingly there is enough amount of the solution outside of the spot. We repeatedly observed that solution flowed back to the focal point when the laser irradiation was

terminated. It obviously indicates that the dry spot is formed by surface lowering and touching the bottom dish surface.
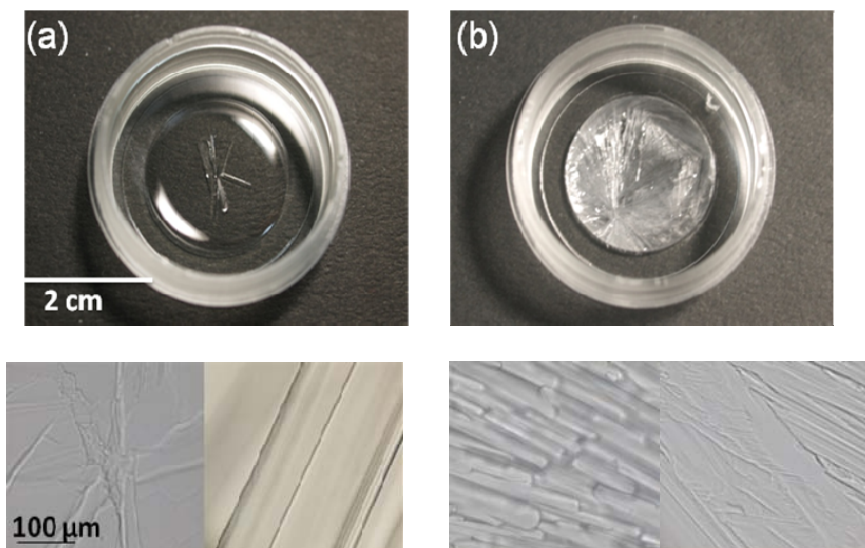
Fig. 3.3 Crystals induced (a) by focused irradiation and (b) by solvent evaporation.

3.2 Crystallization probability: Laser power and solution concentration dependences

The probability of crystallization (forming the flat crystal) was examined by varying trapping laser power and solution concentration. All the measurements were done for 20 minutes and repeated at least 10 times for each condition. For concentration dependence experiments, sample solutions with lower supersaturated value were mainly employed because we could not avoid spontaneous crystallization which is occurred easily in highly saturated solution.

Fig. 3.4 shows results of concentration and trapping laser power dependence. Examined

concentration range is from 5.2 to 6.5 M which corresponds from 0.83 to 1.03 in supersaturated value. Supersaturated value is defined as the ratio of the weight of dissolved solute to that of the solute equals to 1.0 (1.9 g/mL for proline) [6]. Although we examined unsaturated to supersaturated condition, obtained results did not show obvious concentration dependence. Crystallization probability ranging from 40~65% indicates negligible concentration dependence.
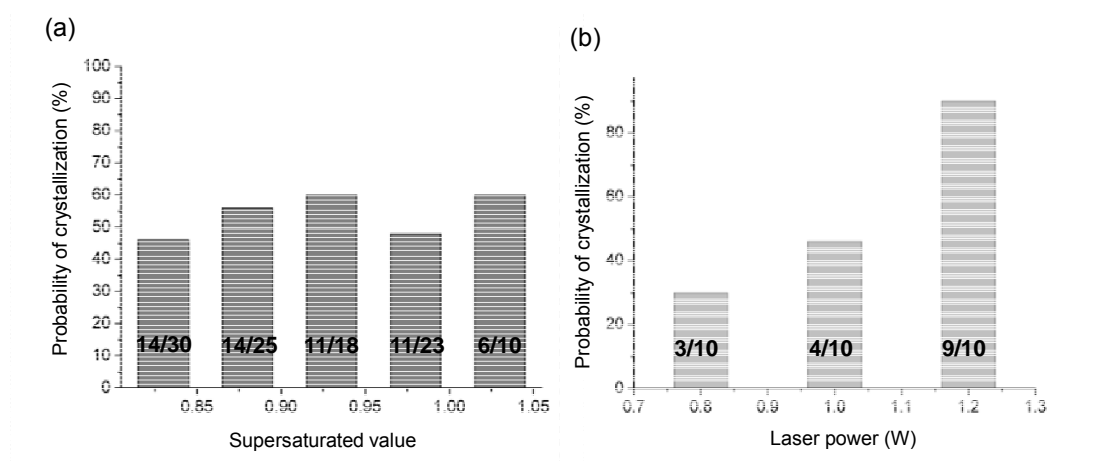
Fig. 3.4 (a) Concentration and (b) power dependence on crystallization probability of L-proline in D$_2$O. Concentrations were 0.83, 0.88, 0.93 0.98 and 1.03 SS under fixed laser power (1 W). Power dependence measured at 0.8, 1.0 and 1.2 W. Supersaturated value was 0.83 SS. Raw values of crystallization probability were mentioned at the bottom each bar.

On the contrary, crystallization probability showed obvious power dependence. It showed drastic probability change from 30% at 0.8 W to 90% at 1.2 W as shown in Fig. 3.3. We will discuss on this point more detail in chapter 3.4.

3.3 Mechanism: Dry spot formation resulting in no crystallization

Here we consider possible process of dry spot formation. Actually, we observe similar local small dry spot by focusing the trapping laser into various solvents which are frequently used in laser trapping crystallization such as H_2O, D_2O, ethanol and deuterated ethanol. For example, Fig. 3.5 shows solution height change when 1.0 W trapping laser was focused to neat D_2O surface. It showed very fast height decrease and then resulted in a dry spot formation; in this case surface reached to the substrate and formed the dry spot just only 12 seconds after starting irradiation.

Because tight focusing of intense laser to the solution induces local temperature elevation due to the absorption of irradiated light by molecules. It induces lowering of surface tension at surroundings of irradiated area, local deforming of surface and Marangoni convection [3-5]. Continuous focusing of the laser to the sinking surface leads further submerging of the surface and the solution surface eventually reaches to the substrate surface.
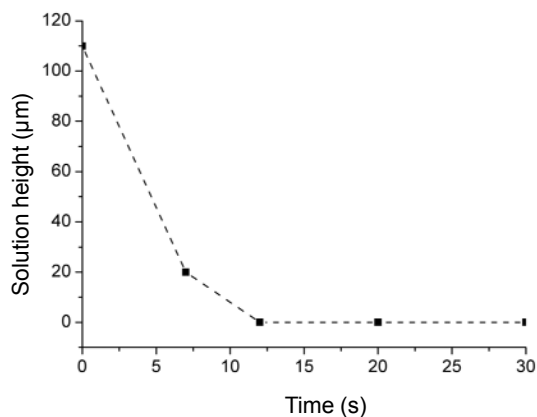
Fig. 3.5 Local solution surface height change of neat D_2O solution by giving 1 W laser to the air/solution interface.

However, it should be noted that dry spot formation induced by focused laser is not normally observed in high concentration solution. Solute molecules are trapped by photon pressure and local concentration will be increased. As a consequence of concentration increase surface tension [7] and refractive index of focused area increases [8], leading to enhance trapping of molecules. Based on these effects, solution was pulled into this area, and eventually solution height started elevating instead of forming the dry spot.

So, local dry spot formation probably means that concentration increasing is not enough attained in that area. Strong interactions between proline and water molecule has been confirmed from Raman spectroscopy [9, 10]. The aggregates of proline cannot be easily formed under such strong proline-water interaction even when photon pressure can efficiently collect molecules. Generally, solvent molecules are too small to be trapped and flow away from the laser spot. Proline molecules join to the movement of D_2O molecules and escaped from focused spot due to strong interaction between them. Therefore it results in forming the dry spot with the process shown in Fig. 3.6.

No crystallization was observed before solution became to be very thin layer. In addition, photon pressure works poorly to the aggregations of L-proline. Laser-induced local temperature elevation and high viscosity of solution (compare to glycine solution) [10] can be considered as negative factors which reduce crystallization probability. Generally higher temperature gives higher solubility. Local heating will increase solubility, resulting in

lowering of supersaturated value [6]. Higher saturation is commonly required for crystallization, therefore, temperature elevation works on a negative factor for crystallization.
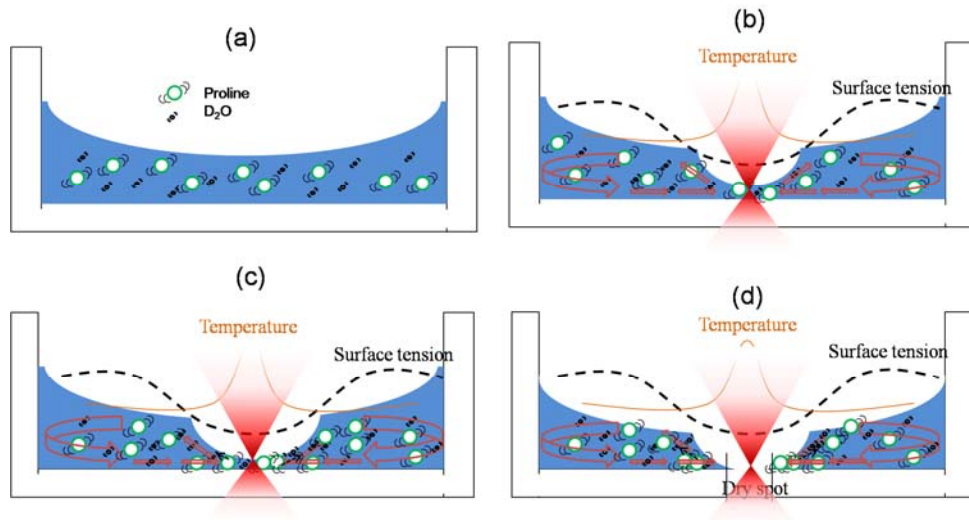
Fig. 3.6 Schematic representation of local dry spot formation. (a) Initial solution without laser irradiation. (b) Focusing trapping laser to the air/solution interface causes sinking of the surface by surface tension decreasing and convection flow around the laser spot. (c) Proline and solvent molecules flow into focal spot with convection flow. A few proline molecules are trapped, but most of them are flowed away. (d) Continuous change of the solution height makes surface reached to the substrate surface and finally solution is spread to the surroundings and forms a dry spot.

Furthermore, higher viscosity of solution makes diffusion of molecules slower. It deteriorates mass transfer of solute molecules from the outside of focal point to trapping area. Efficient nucleation and crystal growth need continuous supply of molecules to keep local concentration sufficiently high around the focal point. However, decreasing of the amount of molecules due to viscosity increase may prevent it. Therefore high viscosity of

solution lowers nucleation and crystal growth rate. On the other hand, lower diffusion rate under higher viscosity can be considered as a positive factor for laser trapping crystallization. Slower diffusion may prevent distrapping of trapped molecules in a trapping volume. However we did not observe crystal formation before solution height became very thin so that this positive factor may not effective.

3.4 Mechanism: Flat crystal formation at thin solution layer

By taking into account above discussion, we propose the flat polycrystal formation process as follows. Since crystallization took place just only before the dry spot formation, its process is complicated due to limited space for molecular movement, thermal capillary effect, evaporation of solvent ,and weak photon pressure effect. Proposed crystallization process is shown in Fig. 3.7. After starting irradiation, L-proline molecules are collected by photon pressure but poorly. Evaporation and mass transfer are enhanced along with solution deformation. Although trapping efficiency could be increased by one or two orders of magnitude by enhanced mass transfer [5], it is still poor in this case as above mentioned. Until the drying is completed, rapid decrease in the volume of the thin layer and dramatically elevated thermal capillary force lead to the accumulation of molecules.

Probability of crystallization is found to be proportional to the laser power. Photon pressure force is increased with laser power, while it also induced temperature elevation that

41

enhanced thermal capillary force and the rate of decrease in space. As a result sudden

decrease of space and drastic elevation of thermal capillary convection are regarded as main

contribution of crystallization, indeed we observed crystallization only occurred just before

dry spot formation. Flat crystal shape and fast growth rate may reflect high concentration in

thin solution layer.
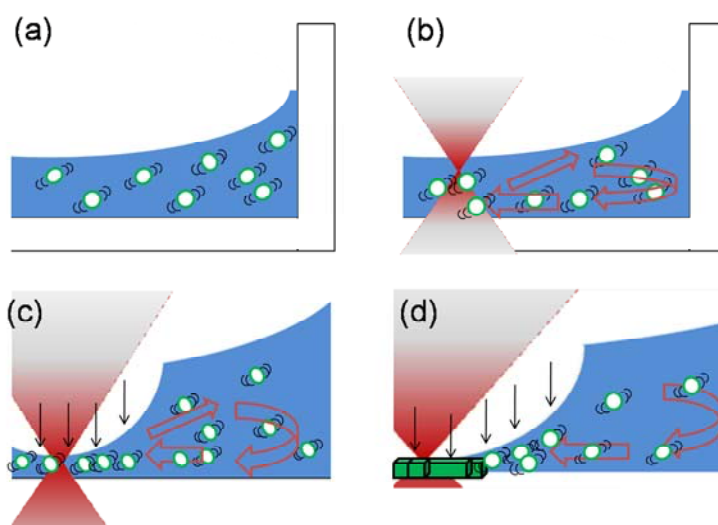
Fig. 3.7 Illustration of proposed crystallization process. (a) Initial solution before laser irradiation. (b) Focus the trapping laser to the air/solution interface and trap small numbers of proline molecules. (c) Thermal capillary force and drastic decrease in space resulting in an accumulation of molecules. (d) Crystallization. (c) and (d) are magnified view around the focal point.

We did not see clear concentration dependence on crystallization as seen in Fig. 3.4a. It is

interpreted that the examined concentration range was too narrow to see the effect for

capillary force and space diminution. Thus we did not see clear concentration dependence.

3.5 Crystal growth and dissolution by trapping laser irradiation near the crystal

As mentioned in the previous section, it was difficult to form single crystal of proline with laser trapping crystallization method in D_2O solution. Here, we examined spatial control of crystal growth by laser trapping. Crystals were prepared by conventional spontaneous crystallization method from 1.1 SS proline/D_2O solution. Crystals taken from mother solution were dropped on cover glass and left for 30 min to stabilize the sample solution with a cover. 1.0 W of trapping laser was focused to a certain point nearby the crystals. We found interesting difference by focusing the trapping laser to aged and newly formed crystal. Aged crystals were formed in mother proline/D_2O solution and the growth already stopped, but latter formed after transferring the solution to the sample container and crystal growth is recognizable although growth rate is not very fast (growth rate is about < 1 µm/min).

When trapping laser was focused to the close vicinity of the aged growth-stopped crystal, we observed the dissolution during trapping laser irradiation and crystal reformation after shutting down the laser as seen in Fig. 3.8. Interestingly, dissolution occurred independent to crystallographic axes (Fig. 3.8b) but formation reflected original axes of the dissolved crystal (Fig. 3.8c). The dissolution is considered as a result of solubility increase caused by temperature elevation. A shape of dissolved crystal suggests isotropic heat dissipation from

the laser spot. Meanwhile after laser off, temperature and solubility lowered and saturation became higher again. Thus molecules are adsorbed to the step and edge of the plane of the crystal and new crystals formed showed sharp edges which reflecting crystal axes (Fig. 3.8c and d).
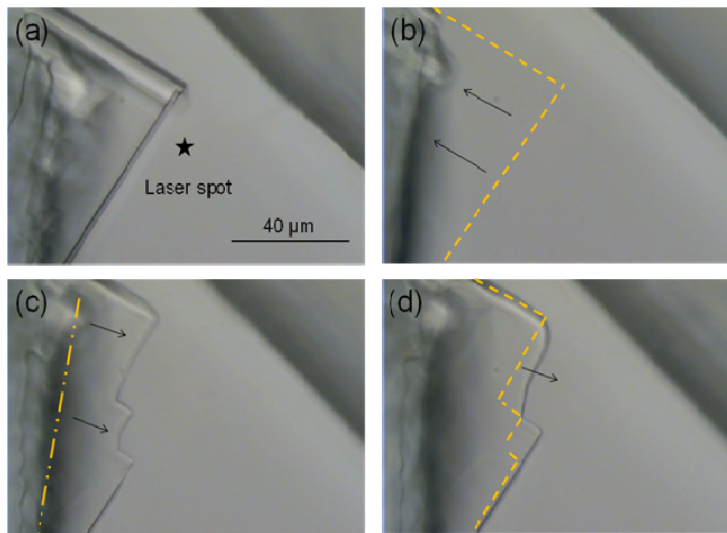
Fig. 3.8 (a) Initial crystal shape before laser irradiation and (b) after started irradiation. Irradiation caused dissolution of crystal. (c) Crystal formation after terminating laser irradiation. (d) Further growth of new crystal. Slight curvature of growth front line is considered due to the dissolution. Yellow dashed lines indicate original shape before changing irradiation condition.

On the contrary, irradiation of trapping laser near the newly formed growing crystal showed enhanced crystal growth as seen in Fig. 3.9. As shown in Fig. 3.9b it shows directionality for enhanced growth. The crystal showed very fast growth along the direction indicated in blue arrows but slow growth along the orthogonal direction (Fig. 3.9b). Preferential crystal growing along the blue arrow-indicated direction seems like 2D and flat growth, which is similar to the surface crystal obtained in solution although the crystal is

fully inundated in solution. Continuous laser irradiation caused further growth (Figs. 3.9b ~3.9d). When the crystal grew continuously and crossed the position of laser spot, we observed slight dissolution of crystal around the laser spot (Fig. 3.9c). It is considered due to the temperature elevation, but dissolution was not so obvious in contrast to aged crystal. The reason is not cleared yet, but new crystal formation requires higher concentration and inhomogeneous local high concentration near the crystal can be suggested.
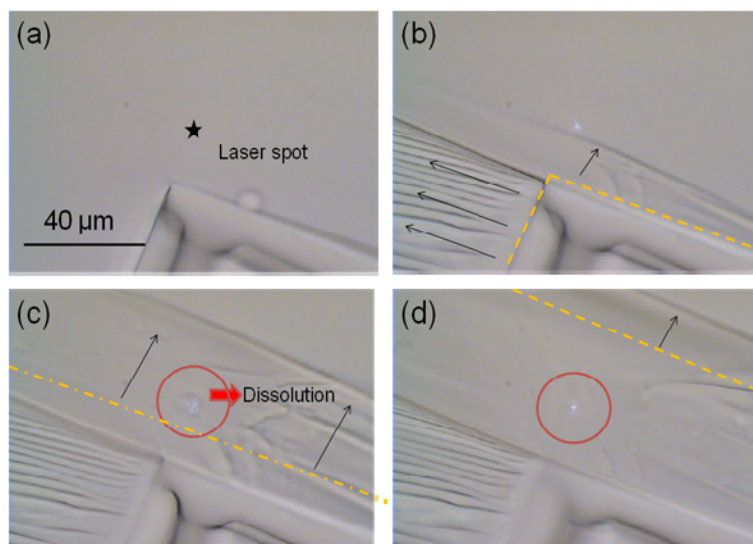
Fig. 3.9 (a) Initial crystal shape. (b) Laser on, induced crystal growth mainly along the original direction. (c) and (d) show further crystal growth and its local dissolution near laser spot.

3.6 Summary

By focusing trapping laser to the air/solution interface, photon pressure and heat generation are induced. Heating caused decrease of surface tension made solution surface deformed. Slower surface deformation than that of glycine/D_2O solution is ascribed to

higher surface tension of solution surface due to walled container shape and resistance of high viscosity Further irradiation after solution height became quite near to the bottom glass substrate gave two results; one is flat polycrystal formation and another is local dry spot formation.

Crystallization always took place when solution deformed to very thin (<5 μm). We consider major driving forces for flat polycrystal formation are thermal capillary force and drastic decreasing of molecular moving space, although quite complex reasons for the crystallization is considered. Probability of crystallization is proportional to laser power but poorly correlated with solution concentration.

Low collection efficiency of molecules by photon pressure, which reflected in poor crystal formation probability, can be attributed to strong interaction of solute and solvent molecules which makes difficult to trap solute molecule. Local dry spot formation is interpreted as a result of coupled movement of solvent and solute molecules from the laser spot.

3.7 References

1. T. Sugiyama, T. Adachi, and H. Masuhara, *Crystallization of Glycine by Photon Pressure of a Focused CW Laser Beam.* Chemistry Letters, 2007. **36**: p. 1480-1481.

2. E.J.G. Peterman, F. Gittes, and C.F. Schmidt, *Laser-Induced Heating in Optical Traps.* Biophysical Journal, 2003. **84**: p. 1308-1316.

3. G.D. Costa and J. Calatroni, *Transient deformation of liquid surfaces by laser-induced thermocapillarity.* Applied Optics, 1979. **18**: p. 233-235.

4. G.D. Costa, *Optical visualization of the velocity distribution in a laser-induced thermocapillary liquid flow.* Applied Optics, 1993. **32**: p. 2144-2151.

5. O.A. Louchev, S. Juodkazis, N. Murazawa, S. Wada, and H. Misawa, *Coupled laser molecular trapping,cluster assembly, and deposition fed by laser-induced Marangoni convection.* Optics Express, 2008. **16**: p. 5673-5680.

6. M. Jelifiska-Kazimierczuk and J. Szydlowski, *Isotope Effect on the Solubility of Amino Acids in Water.* Journal of Solution Chemistry,, 1996. **25**(12): p. 1175-1184.

7. K. Kar and N. Kishore, *Enhancement of Thermal Stability and Inhibition of Protein Aggregation by Osmolytic Effect of Hydroxyproline.* Biopolymers, 2007. **87**: p. 339-351.

8. E. Romano , F. Suvire, M.E. Manzur, S. Wesler, R.D. Enriz, and M.A.A. Molina, *Dielectric properties of proline: Hydration effect.* Journal of Molecular Liquids, 2006. **126**: p. 43-47.

9. P. Zhang, S. Han, Y. Zhang, R.C. Ford, and J. Li, *Neutron spectroscopic and Raman studies of interaction between water and proline.* Chemical Physics, 2008. **345**: p. 196-199.

10. B. Schobert and H. Tschesche, *Unusual solution properties of proline and its interaction with proteins.* Biochimica et Biophysica Acta, 1978. **541**: p. 270-277.

4. Laser Trapping Crystallization of L-proline in Mixed Solvent (D$_2$O & EtOD)

According to the last chapter, crystal formation in D$_2$O by laser trapping is quite difficult for L-proline. As we suggested that strong interactions between solute and solvent molecules may prevent efficient crystallization. We can expect better crystallization probability by changing the solvent, therefore, we examined different solvent for proline crystallization by laser trapping.

Decrease in a solubility of proline by changing or adding other solvent may make higher probability of cluster formation due to increasing in interactions of solute/solute molecules, leading to the higher probability of laser trapping crystallization. Here we chose deuterated ethanol, EtOD, as an additional solvent. We used not ethanol but deuterated ethanol in order to suppress temperature elevation due to the absorption of trapping laser light. The mixed solvent of D$_2$O and EtOD (0.4 g proline, 200 μL D$_2$O + 400 μL EtOD, supersaturated value for this mixed solvent is unknown) is employed for trapping experiments. The solution was dropped to a cover glass and places a cover to prevent evaporation. Crystallization was examined by focusing trapping laser to the air/solution interface.

4. 1 Solution surface height change and crystallization

By giving irradiation, solution surface height was continuously elevated despite a local heating took place as shown in Fig. 4.1. Solution height was simply elevated to twice of initial height. It should be noted that lateral size of solution shrank during irradiation. Solution covered whole substrate surface before irradiation as Fig. 4.2a but its size became smaller after starting irradiation as seen in Fig. 4.2b. It is considered due to fast evaporation of EtOD. Proline/EtOD has lower viscosity and surface tension than proline/D_2O [1]. It can be easily confirmed by dropping both solutions on the glass substrate. EtOD solution of proline forms widely spread thin solution layer, but D_2O solution forms deformed hemisphere on the substrate. After the evaporation of EtOD, viscosity of solution became higher since the solution consists less EtOD. Thus elevation of solution height is explained due to the surface energy and viscosity change induced droplet shape change.
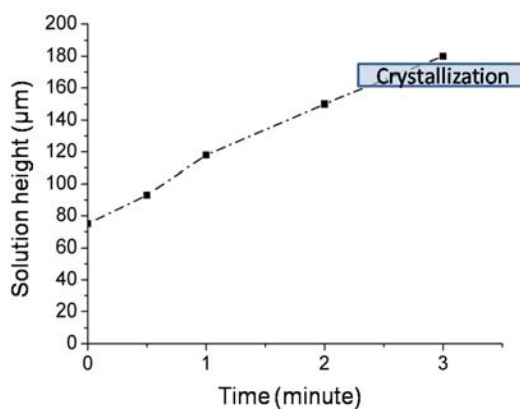
Fig. 4.1 Solution height change recorded during irradiation of 1 W trapping laser.
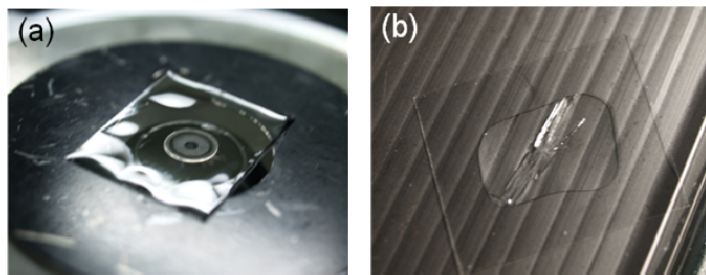
Fig. 4.2 Mixed solution (a) before and (b) after trapping laser irradiation. Solution size was shrunk in (b).
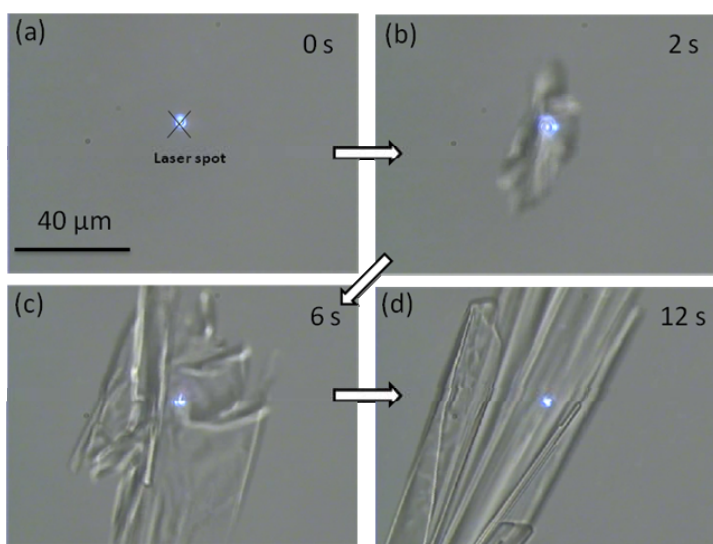
Fig. 4.3 Pictures of crystal formation and growth. (a) Before crystallization, (b) 2 s, (c) 6 s, and (d) 12 s after starting crystallization. Quite rapid crystal growth was observed.

Subsequently we observed crystallization as seen in Fig. 4.3a to 4.3d. Crystal grew longer than 100 μm within 10 seconds. Its crystal growth rate is between that of polycrystal in D_2O and that of single crystal in EtOD (see Chapter 5). Polycrystals were usually formed and the rate of crystal growth was relatively fast. We frequently observed unstably trapped small particles around the laser spot before crystallization. It is probably an aggregate or cluster of proline molecules that trigger the crystallization.

4. 2 Complicated crystallization behavior

From the Fig. 4.2a we can find the solution surface is quite rough. It implies high inhomogeneity of distribution of molecules in solution. In addition, we can guess that solution property such as viscosity, ratio of D_2O to EtOD and surface tension were changing quite a lot during the irradiation. So we regard this crystallization as very complicated behavior and it is difficult to investigate. For example, the ratio of D_2O to EtOD is probably not constant anywhere and it determines the supersaturated value and crystallization can occur or not. Laser irradiation not only induces the photon pressure but also heating. Heating probably induced huge solvent ratio change and inhomogeneous mixing of both solvent molecules even right after preparation of the sample can be suggested. Solubility of proline in D_2O is 100 times higher than that of EtOD (EtOH) [2, 3]. If there is inhomogeneous segregation of D_2O and EtOD during irradiation, huge difference of solubility can cause drastic saturation elevation and result in crystallization.

Even contributions of thermal capillary or volume compaction, which are important for the crystallization in D_2O, are considered less effective for crystallization in mixed solution because no thin layer was formed in mixed solution. Additionally photon pressure probably works more efficiently since interaction of solute and solvent is weak. However, it is still regarded as complex contribution of crystallization as we mentioned.

Although organized understanding of crystallization dynamics and mechanism is difficult,

crystallization in mixed solvent always occurred at the focal spot and crystals were trapped and growing. It is quite alike a typical behavior of laser trapping crystallization. This strongly indicates that decreasing a solubility of proline will give higher probability of laser trapping crystallization. Based on this assumption, we intend to shift the experiment to pure EtOD solvent.

4. 3 Summary

In contrast to D_2O solution case, surface height was continuously elevated and subsequently crystal was formed by focusing trapping laser to the air/solution interface of mixed solvent. Crystallization at higher solution height suggests that different mechanism of crystallization unlike to proline in D_2O.

Even though observed crystallization is similar to that observed in laser trapping crystallization of glycine in a sense of non-drying crystallization, crystal formation in mixed solvent seems more complicated and difficult to elucidate mechanism. Although understanding of crystallization in mixed solution is in progress and we need more experiments, mixed solution results gave very important suggestion: We may improve the probability of laser trapping crystallization by decreasing the solubility with varying solvent.

4. 4 References

1. G. Vhquez, E. Alvarez, and J.M. Navaza, *Surface Tension of Alcohol + Water from 20 to 50 "C.* J. Chem. Eng. Data, 1995. **40**: p. 611-614.
2. M. Jelifiska-Kazimierczuk and J. Szydlowski, *Isotope Effect on the Solubility of Amino Acids in Water.* Journal of Solution Chemistry, 1996. **25**(12): p. 1175-1184.
3. H.D. Belitz, W. Grosch, and P. Schieberle, *Food Chemistry* 2009: Springer.

5. Laser Trapping Crystallization of L-proline

in Deuterated Ethanol (EtOD)

In this chapter we examine laser trapping crystallization in EtOD solution. As we mentioned in previous chapter, proline is known to show moderate solubility to ethanol (EtOH, 0.012 g in 1 ml of EtOH) [1] and can form a single crystal from its solution [2]. It suggests that comparatively weaker solute-solvent interaction in ethanol may allow stronger solute-solute interaction compared with that in D_2O. Thus we can expect higher probability of primal liquid-like cluster formation We can anticipate more efficient collection of this liquid-like cluster, and hence following crystallization under photon pressure of trapping laser.

Based on concepts as mentioned above, we examined laser trapping crystallization of proline in deuterated ethanol. As well as in the case of aqueous solution, we used deuterated solvent in order to suppress temperature elevation due to the absorption of trapping laser light. Similar experimental conditions such as trapping light and initial solution height were set as same as in mixed solvent case. We applied flat substrate, i.e. non-walled condition, in EtOD solution experiments. Sample solution was dropped on the cover glass to form thin layer of the solution. Its thickness was about 100 ~ 150 μm usually. It was covered with a small laboratory dish to suppress solvent evaporation. Trapping laser was focused to the

air/solution interface and kept focusing to the interface during surface height changing.

5.1 Crystallization with surface height elevation

We observed similar crystallization behavior as seen in the case of glycine crystallization [3]. Namely, surface deformation with lowering the surface height was immediately observed by starting laser irradiation and its rate was faster than that in D_2O case. Surface height change during laser irradiation is depicted in Fig. 5.1. After solution height became very low, i.e., at the moment solution layer thickness is very thin, it kept the surface height very low for some moments and then the solution height started elevating gradually. Solution surface height elevation was observed in ~70% of all experiments. Another 30% were resulted in non-surface height elevation as discussed in section 5.2.

The solution height elevation can be due to droplet formation. Indeed, highly dense liquid droplet formation and following crystallization was reported in glycine D_2O solution under laser trapping [3]. We observed similar droplet formation in laser trapping crystallization of proline in EtOD. A boundary of droplet was observed after solution became very thin as shown in Fig. 5.2a. It indicates droplet formed due to local liquid-liquid phase separation as well as in glycine case [3]. Blue spot in Figs. 5.2 is a spot of 488 nm laser that used focus position indicator. Figs. 5.2b and c show growth of dense droplet. Phase boundary of droplet is indicated with dashed line in Fig. 5.2b. A few tens of seconds later, phase boundary

moved to the left side of dotted line. Droplet size became larger slowly with solution height elevation by continuous irradiation of trapping laser, and eventually crystallization was observed. Both single crystal and polycrystal were observed. Fig. 5.3 shows CCD image of typically observed needle-like single crystal which formed with a rate of 10%. We will discuss about polycrystal formation later in section 5.4.
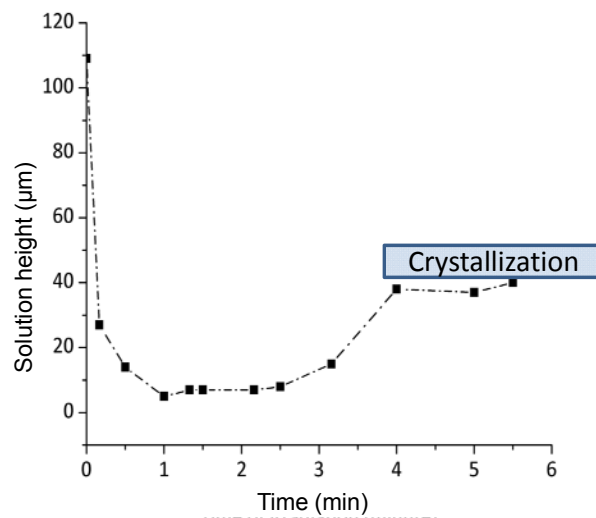
Fig. 5.1 Local solution height change during laser irradiation. Height was first lowered and becoming thin. After kept very thin condition, height was elevated and eventually showed crystal formation. Above curve was obtained with 1.2 SS solution. Laser power: 1.0 W.
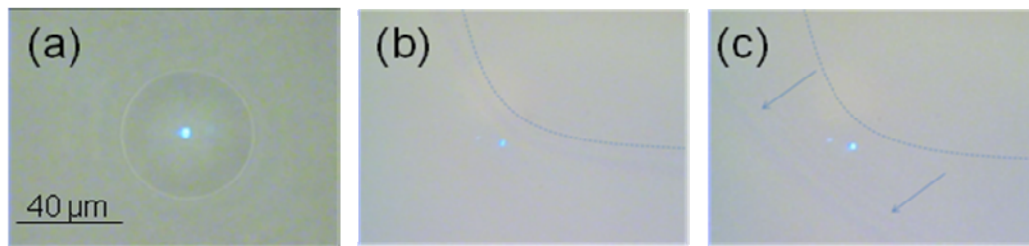
Fig. 5.2 Boundary of droplet observed under microscope. (a) Initial droplet formation at the focal spot, (b) droplet located at the corner of screen and (c) moving of boundary due to an expansion of droplet.
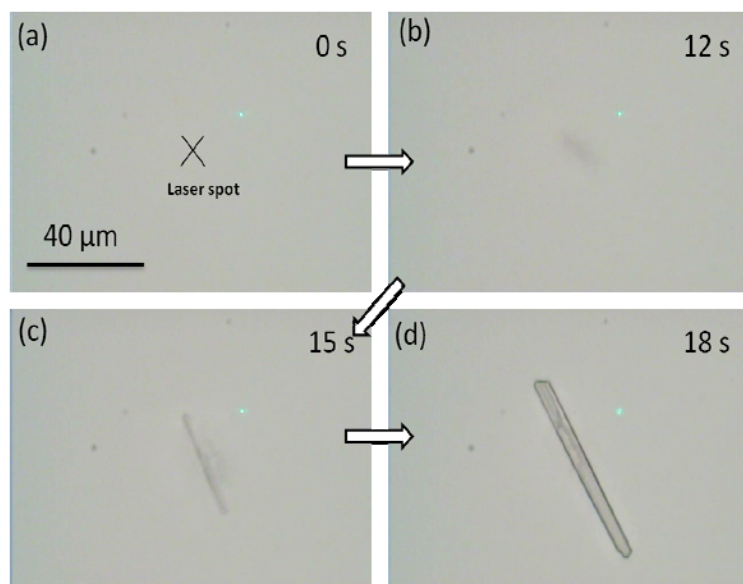
Fig. 5.3 Bright field image of proline crystal induced by focused laser after solution height elevation started. Zero second corresponds to 5 min in Fig 5.1. Crystal formed from 1.2 SS solution. Laser power was 1.0 W.
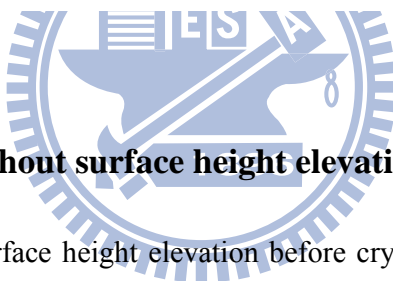
5.2 Crystallization without surface height elevation

We usually observed surface height elevation before crystallization of proline in EtOD. However, above mentioned crystallization process such as surface height lowering, forming very thin solution layer, surface height elevation and eventual crystallization was not always fulfilled. We sometime observed the crystallization during solution height decreasing process without height elevation as seen in height change trajectory depicted in Fig. 5.4. Under applied experimental conditions (supersaturated value: 0.7 ~1.5 SS, laser power: 0.6~1.2 W, solution container: flat glass substrate) the percentage of crystallization without surface height elevation is approximately 30% out of all crystallization. A quality of

obtained crystal was poor as seen in Fig. 5.5b and crystals were polycrystalline.
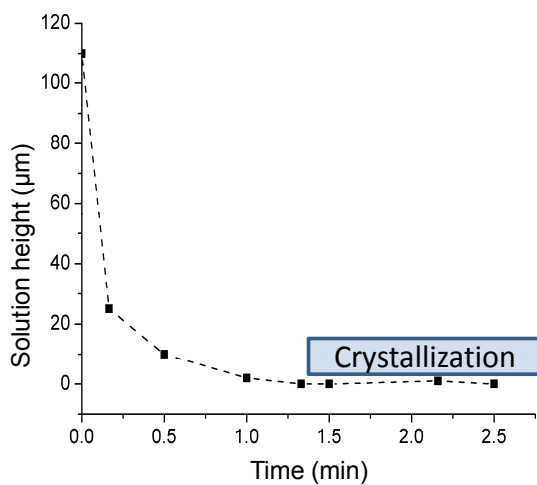
Fig. 5.4 Local solution height change by trapping laser irradiation. Solvent dried and it did not show surface elevation. Crystal was formed without height elevation. Supersaturated value was 1.0 SS. Applied laser power was 1.0 W.
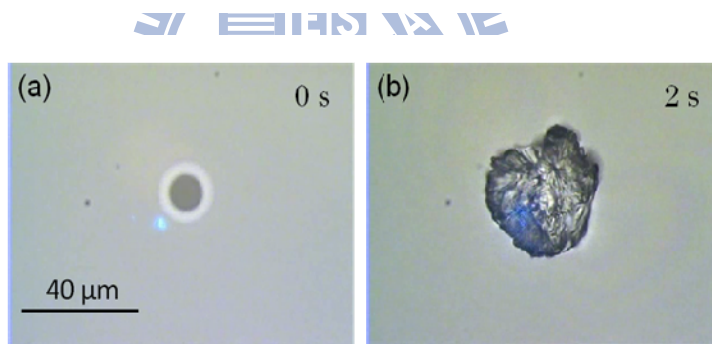
Fig. 5.5 Typical crystal structure formed without solvent height elevation.

Actually this behavior without solution surface elevation was frequently observed in higher power range. Fig. 5.6a shows the laser power dependence of dry crystallization probability. As we mentioned previously, concentration increase to very high range can induced surface elevation because of surface tension increase. If we assume that solution surface elevation is determined by local concentration, laser power dependence of

crystallization without surface elevation can be explained by considering two laser power

dependent factors; necessary time to rupture solution layer and optical trapping rate under

photon pressure which represents number of trapped molecules during unit time [4].
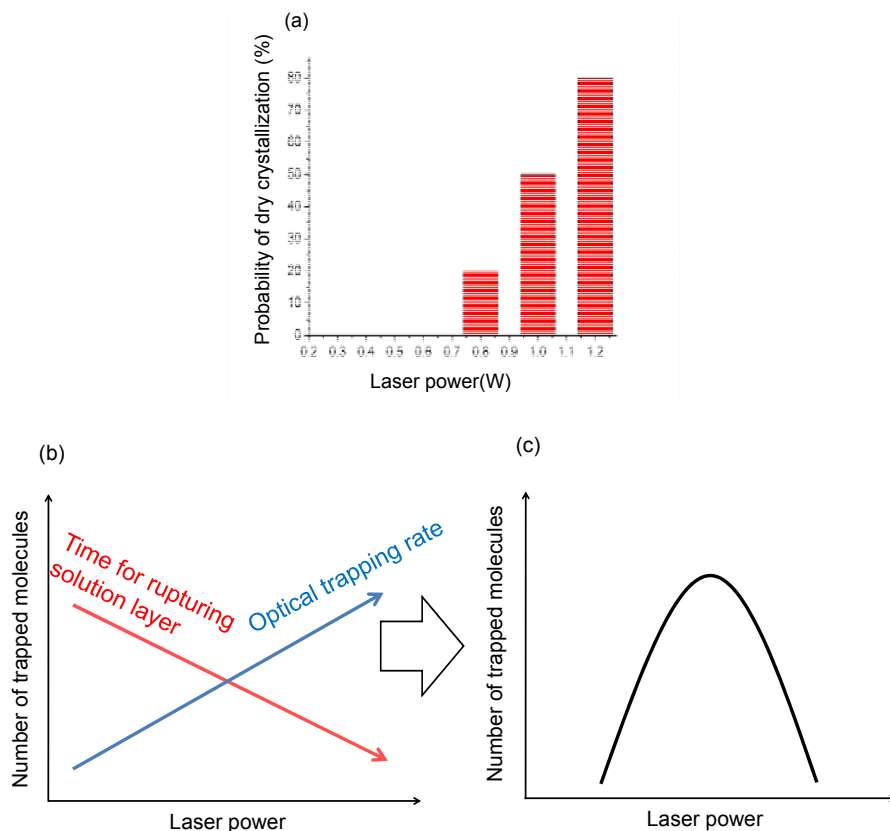
Fig. 5.6 (a) Probability of crystallization without solution surface elevation. Sample is proline/EtOD. Supersaturated value is 1.0~1.5 SS. (b) Schematic drawing of laser power dependent number of trapped molecules before rupturing solution layer and crystallization. Red and blue lunes indicate necessary time to rupture solution layer and optical trapping rate under photon pressure, respectively. (c) power dependent number of trapped molecules after considering two factors depicted in (b).

Higher laser power causes higher temperature elevation and results in rapid solution

height lowering as shown in Fig. 5.6b by red line. In spite of stronger photon pressure under

59

high laser power, number of trapped molecule is suggested to be quite small. Thus, concentration can not be high enough to elevate surface height, and showed dry spot formation with rupturing thin solution layer and crystallization without surface elevation.

On the other hand, lower laser power offers much longer time until rupturing of thin solution layer. Although there is enough time to confine molecules in focal spot, photon force is too weak to trap sufficient number of molecules to elevate surface height. As a result, number of trapped molecule is probably represented by a parabolic curve depicted in Fig. 5.6c that is a product of contribution of solution rupture time and trapping rate under photon pressure. Thus, from a comparison with observed crystallization probability depicted in Fig. 5.6a, suitable laser power to avoid the dry spot formation with high efficient trapping is estimated to be 0.6~0.9 W.
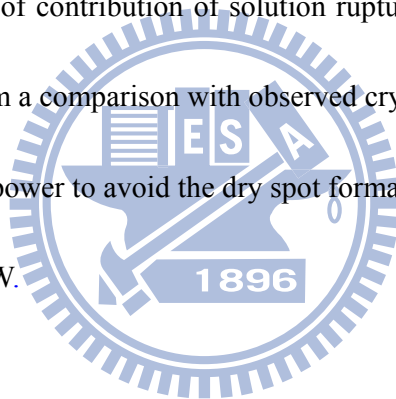
5.3 Crystallization probability: Laser power and solution concentration dependences

We checked sample concentration and trapping laser power dependence of crystallization probability as shown in Fig. 5.7a and b, respectively. In this investigation, samples showed no surface height elevation are excluded for analysis. All the experiments were done for 15 minutes and repeated more than 12 times for each condition. Examined concentration range was from 0.8 to 1.7 M which corresponded from 0.7 to 1.5 SS. As we can see in Fig. 5.7a,

crystallization probability increased with increasing of concentration. It showed very low

probability of 33 % at 0.7 SS, while it became 100% with 1.5 SS. Laser power dependence

(Fig. 5.7b) also showed increase of crystallization probability with trapping power increase.

Trapping power at 1.2 W could achieve 100% crystallization. To the contrary, trapping

crystallization success percentage at 0.6 W was just only 30%.
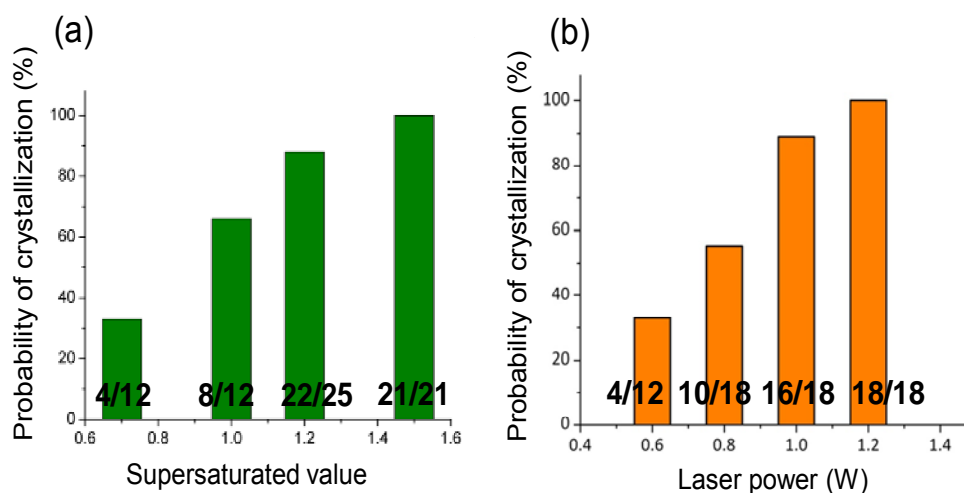
Fig. 5.7 Concentration (a) and trapping power (b) dependence on crystallization probability of proline in EtOD. Applied laser power for concentration dependence was 1.0 W. Supersaturated value of solution used for power dependence was 1.3~1.4 SS.

In contrast to the concentration dependence on crystallization probability observed in

D_2O, EtOD solution showed clear concentration dependence. It strongly suggests that clear

indication of crystallization mechanism is different between in EtOD and D_2O. In D_2O case,

crystallization occurred when the solution thickness was very thin. There is evident

difference between two cases; it is solution height elevation before crystallization. It is

related to the formation of dense liquid droplet, and we have observed dense liquid droplet formation and surface elevation only in EtOD. These results suggest that photon pressure greatly contributed to the crystallization in EtOD under laser trapping. More details will be discussed later.

5.4 Solution surface height and crystallinity

Observed trapping induced crystals are classified into two cases: needle-like single crystal and polycrystal. We found that crystal shape depends on the solution height when crystallization occurred. Fig. 5.8a and b depict the solution surface height when crystallization occurred for single crystal and polycrystal, respectively. It shows that crystallization mainly took place at the solution height around 10-60 μm on both crystals. This value is relatively smaller than that in glycine crystallization case. It might be explained from relatively slow height elevation in proline/EtOD than glycine/D_2O case. Higher temperature elevation in EtOD suppresses local concentration increasing rate. Thus surface elevation rate and height will be slower and lower, respectively, than that observed in glycine/D_2O case [3]. Although concentration increasing rate became lower due to higher temperature elevation, concentration can be sufficiently high to form the crystal in this slow elevation process.
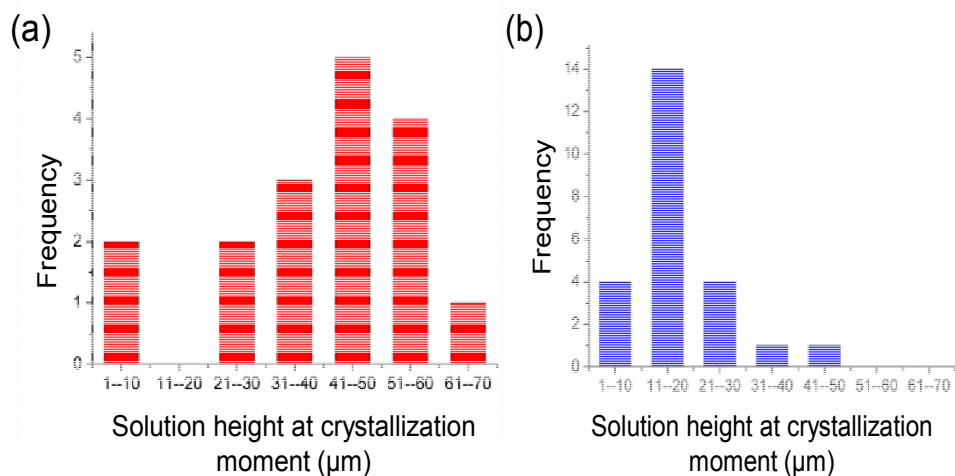
Fig. 5.8 The distribution of solution height at the moment of crystallization for (a) single needle-like crystal and (b) polycrystal. 0.7 ~1.5 SS proline/EtOD solution and 0.6 ~1.2 W laser power used.

From a comparison of solution thickness where single crystal and polycrystal formation took place, single crystal was formed at higher solution surface height. It is reasonable by considering less contribution of quick drying which is more active in thinner solution layer at low surface height. Polycrystal formation was observed more often in thinner solution due to quick drying of solution as well as proline in D_2O. To the contrary, thicker solution has less effect of drying for crystal formation. Solution height elevation occurred with the formation and growth of high dense liquid droplet. Thus proline molecules in high dense liquid droplet at higher solution surface will interact strongly each other under photon pressure and result in single crystal formation.

In laser trapping crystallization of proline in D_2O, we did not observe single crystal but always observed flat polycrystal. Contrary proline in EtOD shows single crystal formation

with a yield of 10%.

5.5 Mechanism: Crystallization with solution height elevation

An obvious difference of laser trapping crystallization of proline in EtOD and D_2O is whether the apparent surface height elevation before crystallization is observed or not. We should note that here we consider only crystallization after surface height elevation. As you can see in Fig. 5.1, EtOD solution of proline showed surface height elevation before crystallization.

Actually, crystallization with forming better quality crystal was always observed after surface height elevation and it is deeply related with high dense droplet formation. In other word, the single crystal formation is always observed through the droplet formation. Temperature elevation due to laser irradiation increases the solubility and lowers saturation degree, which are inappropriate conditions for crystallization. However we could crystallize L-proline in EtOD under such conditions. We suggest that droplet formation is necessary process for achieving local and transient concentration increase for laser trapping crystallization.

Droplet formation is induced by many factors such as local temperature elevation, decreasing of surface tension, Marangoni convection [5-7] and photon pressure [3, 8]. Here we quickly overview the crystallization through the droplet formation. More details will be

discussed in next chapter. Possible explanation on crystallization through the droplet formation is as follows. Fig. 5.9 schematically depicts the crystallization process through the dense liquid droplet. The formed droplet is consisted of molecules and clusters. Although concentration is high in the droplet compared with surrounds, still interactions between molecules are not so strong (Fig. 5.9a). Molecules are continuously collected by continuous laser trapping and condensed at the focal spot by photon pressure as shown in Fig. 5.9b. Enhanced interaction stimulates more interaction of molecules and clusters. Finally crystal is formed.
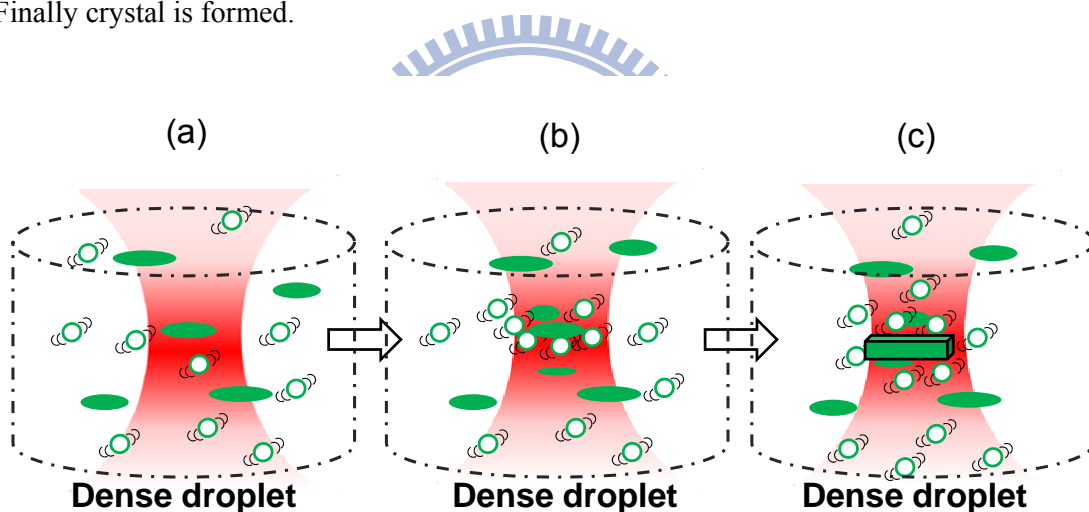
Fig. 5.9 Crystallization process in dense liquid droplet by laser trapping crystallization. (a) Molecular clusters and aggregates in droplet. Interaction is not so strong. (b) Condensation and collection of them by photon pressure. (c) Crystallization.

Laser trapping crystallization of proline in EtOD is quite similar to that of glycine in D_2O [9]. It is reported that laser trapping crystallization of glycine/D_2O by focusing trapping laser to the surface shows the same solution height change, i.e. thinning, forming very thin layer and height elevation, and crystallization with very interesting dense liquid droplet

formation. It suggests that observed L-proline crystallization could be interpreted as laser trapping crystallization.

5.5 Microscopic characterization of crystals

Formed crystals were observed polarization microscopy under crossed Nicole condition to confirm crystallinity. Analyzer and polarizer were orthogonally oriented across a specimen in crossed Nicole microscope. Almost, crystalline materials are birefringent where the light split into two beams and travels in different directions at different speeds. Non-birefringent materials such as amorphous or isotropic liquid give dark appearance by linearly polarized light irradiation under crossed Nicole condition. In contrast, birefringent crystals appear bright under such conditions.

A bright field and corresponding crossed Nicole images of crystal formed by laser trapping are shown in Fig. 5.10a and b, respectively. Whole part of formed crystal obviously appeared as bright object in crossed Nicole image and angle dependent brightness change. These results strongly suggest that it is crystal of proline. Another crossed Nicole image taken with grown the same crystal after growing is shown in Fig. 5.10c. Larger crystal shows clearer contrast in polarization image.
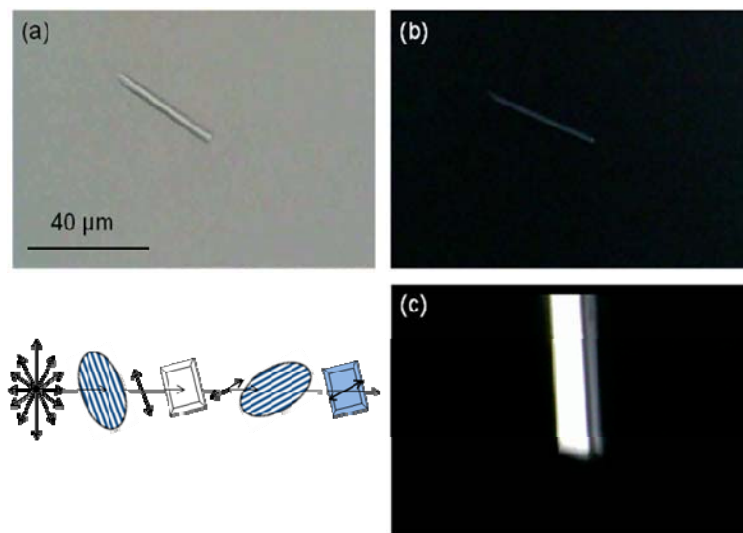
Fig. 5.10 (a) Bright field image of crystal formed by laser trapping. Image taken 5 sec after crystallization started and (b) corresponding crossed Nicole image of (a). (c) Crossed Nicole image of the same crystal grown by laser trapping for 1 min.

In addition to polarization imaging, we examined second-harmonic generation (SHG) from formed crystal. SHG is well known nonlinear optical properties for studying interfaces in physics and chemistry [10-12]. SHG is surface-selective due to the fact that, as second-order processes, they are forbidden under the electric-dipole approximation in a medium with centrosymmetry, but the symmetry is always broken at a surface. Moreover, they are highly sensitive and can readily detect the presence of molecules on a surface at submonolayer densities.

Usually short pulse laser such as picosecond to femtosecond lasers are used for SHG observation. It is surprising that we can observe SHG caused by CW trapping laser. Fig. 5.11 shows observation of SHG signal from trapping-induced proline crystal in EtOD by

focusing a 1 W of trapping laser. The noncentrosymmetry of the proline crystal structure $(P2_12_12_1)$ is regarded as the main reason of SHG. Observed SHG signal showed intensity change following to the rotation of the crystal. It is known that SHG signal intensity varies depending upon matching of the crystal axis and polarization direction of incident laser light.

Polarization microscopy and SH generation suggests formation of single crystalline proline and conservation of single crystalline structure during laser trapping crystallization and growth.
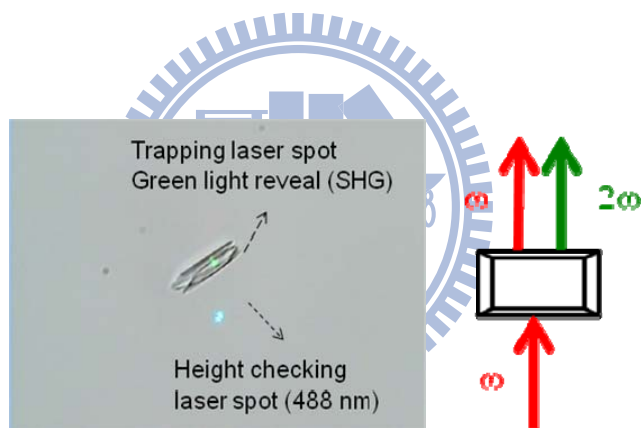
Fig. 5.11 SHG signal observed during trapping crystallization. Light source for SHG and laser trapping was the same 1064 nm laser beam. Trapping laser power is 1.0 W. Green spot in the image is SHG. Blue spot is 488 nm light from diode laser.

5.6 Spectroscopic characterization of crystals

Spectroscopic characterization of proline crystal was examined by Raman scattering measurement. Proline crystals formed by laser trapping in EtOD was not long-lived. The crystal dissolved into solvent by cutting the trapping laser and removing the cover due to its

high hygroscopic nature. To prevent dissolving of the crystal by adsorbing atmospheric water, formed crystals were buried in transparent superglue.

Fig. 5.12 shows experimentally obtained Raman spectra of crystal formed by trapping and commercially obtained powder crystal with Raman spectrum of crystalline proline reported in the reference. Peaks of obtained L-proline crystals' spectra are quite broad and shifted majorly compare with that in literature [13].

1	Ring bending	11	CH_2 twisting, NH_2^+ twisting
2		12	CH_2 bending
3	CC stretching	13	
4	CN bending, NH rocking	14	CH bending
5	CC stretching	15	NH_2^+ wagging, CH_2 bending
6	CC stretching	16	CH_2 bending
7	NH_2^+ rocking	17	NH_2^+ bending
8		18	$CO2^-$ stretching
9	CC stretching		
10	CH2 rocking		
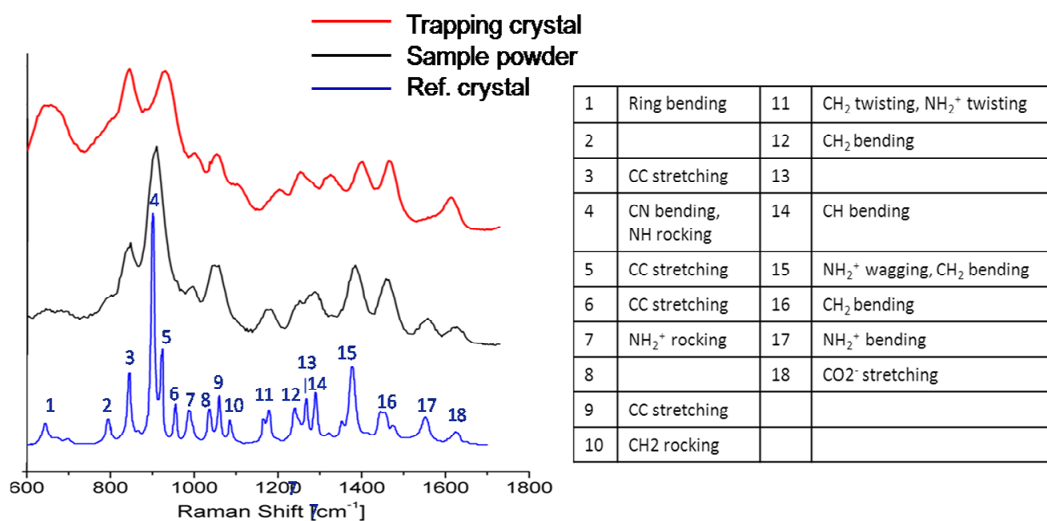
Fig. 5.12 Raman spectra of proline crystal formed by laser trapping crystallization (red), commercial powder (black), and crystalline proline data from reference [13](blue). Table inside figure is assignment of the peaks which is referred from reference [13].

Large shifts are probably due to the difference of D and H exchange because of used deuterated solvent. Since the molecular flexibility is reduced significantly in the crystal, it should show narrower peaks. For example, the intensity of the NH rocking vibration at ~900 cm^{-1} is specially strong for dry proline [14]. However spectrum of trapping-induced

crystal showed quite broad peak. Raman spectrum of commercially obtained dried powder showed sharper peak than that of laser trapping-induced crystal. For this reason we think broader bands in spectra are due to remained solvent in crystals. It makes molecules in the crystal little flexible and spectrum can be broader.

5.7 Summary

Focusing of trapping laser to the air/solution interface induced rapid solution surface deformation. After forming very thin solution layer, giving two kinds of results: Crystallizations along with or without solution surface height elevation. Direct drying crystallization without surface height elevation seemed like drying crystallization as well as a crystallization in D_2O solution case. Formed crystals were only polycrystal. A 30% of crystallizations were this type and frequently observed at higher laser power. Higher laser power induced surface height decrease is too quick to trap enough molecules, and resulted in drying polycrystal formation.

On the other hand, in crystallization occurred after surface height elevation (~70%), we observed single crystals and polycrystals formation. Since we observed crystallization after solution height elevation, thermal capillary force and moving space limitation are considered as recessive reason and photon pressure can be regarded as dominant contribution for crystallization. Probability of crystallization is proportional with laser

power and solution concentration.

Crystallization after surface height elevation was always observed together with the dense droplet formation. We observed clear boundary of droplet under microscope and it grew into millimeter size. Observed droplet formation is very alike with that observed in glycine/D_2O.

Higher temperature elevation induced by laser in EtOD may suppress the droplet formation. Thus droplet formed and grew slowly compare to that in glycnie/D_2O. This slow height elevation is due to slow growth of droplet. Crystal quality depends on the solution height at the moment of crystal formation during surface elevation. Single crystals and polycrystals were formed at higher and lower solution height, respectively. Probability of single crystal formation is about ~10%.

Crystals were confirmed by polarization images, SHG and Raman scattering measurement. These results suggest the formation of proline crystal with defined crystallographic axes.

Observed crystallization dynamics such as surface height change, dense liquid droplet formation and different types of formed crystal are quite similar with that observed in laser trapping crystallization of glycine. It suggests that crystallization of L-proline in EtOD after surface height elevation is induced by photon pressure that caused by trapping laser.

5.8 Reference

1. A. McPherson, *Crystallization of biological macromolecules*. 1999, New York, USA Cold Spring Harbor Laboratory Press.

2. B.A. Wright and P.A. COLE, *Preliminary examination of the crystal structure of l-proline*. Aeta Cryst., 1949. **2**: p. 129-130.

3. K.-i. Yuyama, T. Sugiyama, and H. Masuhara, *Millimeter-Scale Dense Liquid Droplet Formation and Crystallization in Glycine Solution Induced by Photon Pressure*. J. Phys. Chem. Lett., 2010. **38**: p. 1321-1325.

4. Y. Nabetani, et al., *Effects of optical trapping and liquid surface deformation on the laser microdeposition of a polymer assembly in solution*. Langmuir, 2007. **23**: p. 6737-6743.

5. G.D. Costa, *Optical visualization of the velocity distribution in a laser-induced thermocapillary liquid flow*. Applied Optics, 1993. **32**: p. 2144-2151.

6. G.D. Costa and J. Calatroni, *Transient deformation of liquid surfaces by laser-induced thermocapillarity*. Applied Optics, 1979. **18**: p. 233-235.

7. O.A. Louchev, et al., *Coupled laser molecular trapping,cluster assembly, and deposition fed by laser-induced Marangoni convection*. Optics Express, 2008. **16**: p. 5673-5680.

8. K.-i. Yuyama, et al., *Single droplet formation and crystal growth in urea solution induced by laser trapping*. Proc. of SPIE, 2010. **7762**.

9. T. Sugiyama, T. Adachi, and H. Masuhara, *Crystallization of Glycine by Photon Pressure of a Focused CW Laser Beam*. Chemistry Letters, 2007. **36**: p. 1480-1481.

10. T.F. Heinz, *Second-Order Nonlinear Optical Effects at Surfaces and Interfaces*. Elsevier, Amsterdam, 1991.

11. Y.R. Shen, *Optical second harmonic-generation at interfaces*. Annu. Rev. Phys. Chem., 1989. **40**: p. 327-350.

12. K.B. Eisenthal, *Liquid interfaces probed by second-harmonic and sum-frequency spectroscopy*. Chem. Rev, 1996. **96**: p. 1343-1360.

13. J. Kapitan, et al., *Proline Zwitterion Dynamics in Solution, Glass, and Crystalline State*. Journal American Chemical Society, 2006. **128**: p. 13454-13462.

14. P. Zhang, et al., *Neutron spectroscopic and Raman studies of interaction between water and proline*. Chemical Physics, 2008. **345**: p. 196-199.

6. Dense Liquid Droplet

As we described in previous chapter, droplet is formed after solution height started elevating from the thin solution layer. Droplet formation found in EtOD solution is inseparably related to solution height elevation as well as in glycine and urea case [1-3]. Formation dynamics and its role for crystallization are discussed in this chapter.

6.1 Droplet formation and disappearance
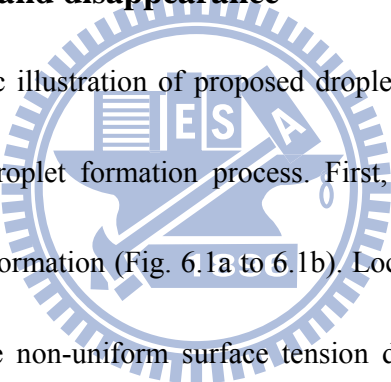
Fig. 6.1 shows schematic illustration of proposed droplet formation dynamics based on experimentally observed droplet formation process. First, laser focusing to the solution surface induced surface deformation (Fig. 6.1a to 6.1b). Local temperature elevation due to laser irradiation caused the non-uniform surface tension distribution, which leads to the surface depression and the following formation of the thin solution layer [4-6]. Proline molecules are efficiently supplied by mass transfer due to Marangoni convection to the focal point, namely a thermocapillary effect. As a result, large clusters are generated due to the increase in the interactions between the molecules, and photon pressure efficiently works on them (Fig. 6.1b). Proline and EtOD molecules are dissociated and subsequently high concentration area of proline molecule, i.e. small high density droplet, is formed around the focal spot (Fig. 6.1c). High concentration area increases the surface tension and

the refractive index, the former pulls the solute molecules into focused area and the latter

enhances photon pressure so that solution height is elevated to form high density liquid

droplet. Eventually, the droplet grows to millimeter size specially by focusing laser to

glass/solution interface (Fig. 6.1d) and can be seen even by eyes as shown in Fig. 6.2.

Formation and growth of the droplet are considered as one of the liquid-liquid phase

separation between photon pressure-induced local high concentration region and

surrounding low concentration region.
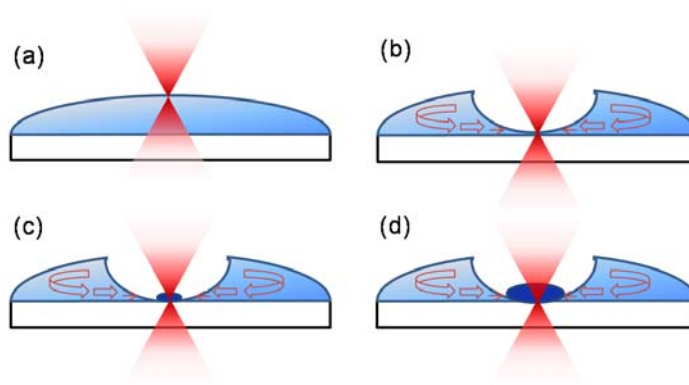
Fig. 6.1 Illustration represents observed droplet formation process. (a) Irradiation to the air/solution interface. (b) Surface deformation due to Marangoni effect and convection flow induced. (c) Efficiently collecting molecule through mass transfer and higher concentration phase was formed.   (d) Grown droplet; large concentration different between droplet and outside of it resulting in liquid-liquid phase separation.
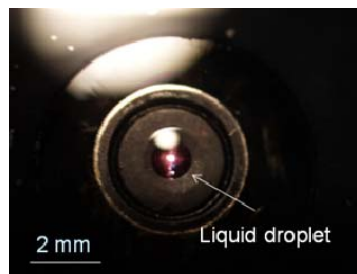
Fig. 6.2 Picture shows millimeter-size liquid droplet. White arrow indicates the place of droplet.

Droplet was maintained for a few tens of seconds even by terminating the trapping laser irradiation. Droplet slowly shrunk and suddenly disappeared with vanishing its boundary. Crystals formed in inside of the droplet slowly dissolved with the disappearance of droplet even it existed in the supersaturated solution. We observed a movement of crystals to the boundary of droplet and started dissolving after trapping laser termination. Pictures shown in Fig. 6.3 represent the change of the same crystal after terminating laser irradiation. One of two crystals observed in Fig. 6.3a was dissolved and disappeared, and another one became smaller than in left picture (Fig. 6.3b).

Trapping-induced glycine crystal in supersaturated solution usually showed continuous growth even irradiation of trapping laser stopped. However, proline crystal formed by laser trapping typically disappeared by dissolution after stopping laser irradiation. This difference can be explained by extreme hygroscopicity of proline. Proline crystal shows highly hygroscopic and even large crystal formed by conventional crystallization method is easily dissolved by atmospheric moisture. Another possible explanation is concentration difference between high concentration droplet and low concentration surroundings. After stopping irradiation, molecular transfer probably occurs at the phase boundary between droplet and its surroundings to equilibrate the concentration of two phases. The concentration of droplet inside continuously decreased to equilibrate with outside, and therefore crystal will dissolved even its in supersaturated solution.

Due to the limitation of our set up, we can record local temporal change of solution as height change but not able to see as surface landscape change. However, the recorded height increasing strongly suggests that bulged surface at the focal point is due to the droplet same as glycine case.
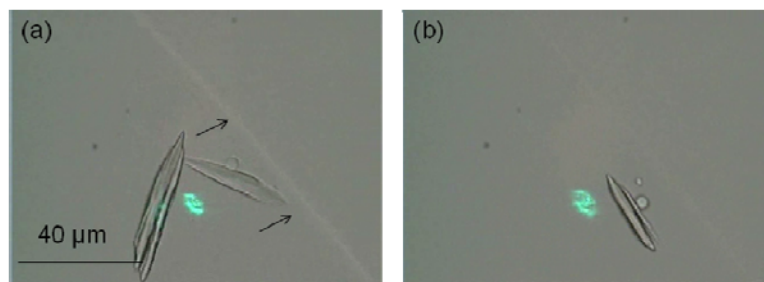
Fig. 6.3 Dissolution of crystals near phase boundary of droplet after shut-down of trapping laser. Crystals before (a) and after dissolving (b). Black arrows indicate phase boundary.

6.2 Importance of droplet formation for crystallization

We should note that crystallization always occurs through the droplet. It implies that inseparable relation between high density droplet and crystal formation.

According to laser trapping crystallization study of glycine in D_2O, crystallization was observed without changing the solution height when the walled container was applied [3]. However, proline/EtOD solution needed surface lowering, elevation and droplet formation to be crystallized even using similar container condition was applied. Fig. 6.4 showed comparison of local surface height change of glycine in D_2O and L-proline in EtOD. Both experiments were done by using the same container. Usage of the walled-container

prevented surface deformation and solution showed no height decreasing in D_2O. In contrast to slight elevation and faster crystallization on glycine in D_2O, proline in EtOD showed very slow height lowering as depicted in Fig. 6.4 with dashed line. After long time irradiation, solution height around laser spot became very thin and formed the dense liquid droplet. It caused solution height elevation with growth of droplet size, and finally we observed crystal formation at the focal spot.
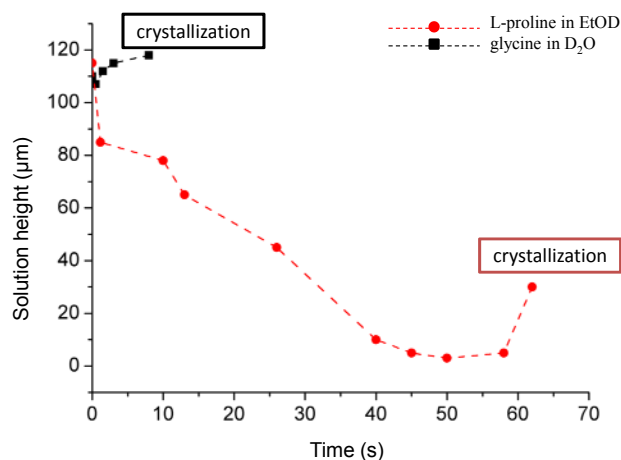
Fig. 6.4 Comparison of local height change during laser trapping between glycine in D_2O and proline in EtOD. Same sample container, cut sample vial, was used for both sample.

This result indicates that thin layer and droplet formation is inevitable for trapping crystallization in proline/EtOD case. It may imply that higher temperature elevation is induced in EtOD so that proline cannot easily be crystallized because increase in solubility and mobility of molecules. However, the molecular movement will be restricted in limited space of solution thin layer and it will help to form liquid-like cluster as nuclei with

achieving efficient trapping and aligning of molecules. We frequently observed unclear shadows of small particles around focal spot during droplet formation. These particles may be flowing to the off-plane of laser focus and, therefore, cannot be seen clearly in microscope images. We consider it as large liquid-like cluster of L-proline molecule that contributes for nucleation in thin layer.

6.3 Droplet formation dynamics with spectroscopy

In order to understand droplet formation dynamics, we measured backward scattering intensity change during laser trapping at the solution surface. Scattering signal intensity reflects concentration and temperature change of proline molecules. For backward scattering measurement, we detected the reflection of 488 nm laser light from the air/solution interface by EMCCD. Intensity trajectory was constructed with plotting laser reflection intensity by taking the laser spot signal on EMCCD image (sum of 22×22 pixels)

Scattering intensity trace is shown in Fig. 6.5. Horizontal and vertical axes are time after starting trapping laser irradiation and accumulated scattering intensity reconstructed from EMCCD images, respectively. Scattering intensity change is explained by a reflectivity (R) at the interface of two different media with equation 6-1, where n_1 and n_2 are the refractive index of L-proline solution and the air, respectively.

$$R = (\frac{n_1 - n_2}{n_1 + n_2})^2 \dots\dots\dots\dots\dots\dots\dots\dots\dots\dots \text{(6-1)}$$

As seen in Fig. 6.5, we observed scattering intensity change around 300 sec which is attributed to the droplet formation. Intensity increased about twice after droplet formation than before of it. We can assume that the refractive index of the air, n_2, is constant during the measurement. Refractive index increase with increase in concentration but decrease in temperature [8].
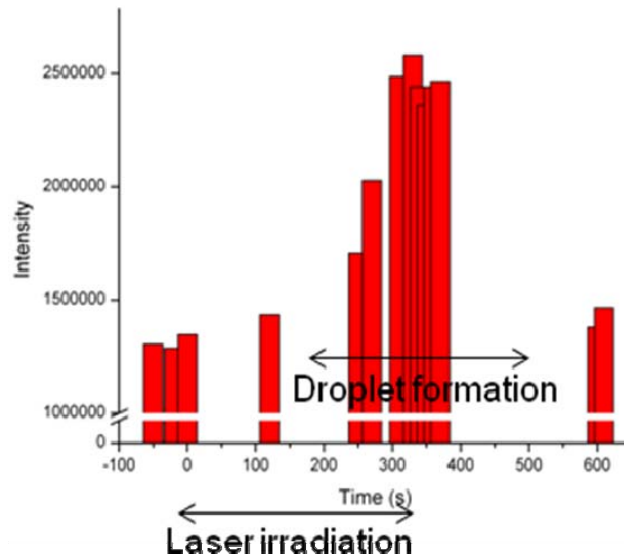
Fig. 6.5 Backward scattering intensity from the air/solution interface reconstructed from EMCCD image during laser trapping.

As shown in eq. 6-1, reflectivity increases with increasing n_1. It means that observed reflectivity increase may due to the increased concentration. We observed high intensity preservation even after stopped focusing trapping laser ($\sim$ 350 s) where the droplet still existed. From this result, we observed scattering intensity change mainly reflected a local

79

molecular number change during laser trapping, and intensity increase is interpreted due to high concentration droplet formation.

6.4 Crystallization through dense droplet

In general, crystallization needs high concentration and high molecular ordering. Fig. 6.6 represents schematic drawing of crystallization process based on a classic nucleation theory where slow increasing in concentration results in crystallization [9]. As explained in the classic nucleation theory, concentration increase induces molecular interaction and ordering simultaneously. Small clusters of ordered molecules interact and increase its size and eventually form crystal with taking sufficiently long time as depicted with dashed line in the figure.

In this work, combination of photon pressure and Marangoni convection flow caused rapid concentration increasing [4-6]. Thus well-ordered molecular arrangement could not be achieved well in short time. Additionally temperature elevation induced thermal disturbance may obstruct molecular ordering. As a result, proline in EtOD probably advanced to form "liquid nucleus" which has poor ordering as depicted in Fig. 6.6 instead of forming ordered clusters. As seen in a phase diagram depicted in Fig. 6.7, rapid increase of concentration induces jump from liquid phase to liquid-liquid separation phase with crossing the solid-liquid coexistent phase [10]. Continuous irradiation to the air/solution interface causes

further elevation of molecular alignment and subsequent phase transition to solid-liquid

coexistent resulting in crystallization. Crystallization in leaser induced high concentration

and temperature area, i.e. in dense droplet, can be explained with this phase diagram
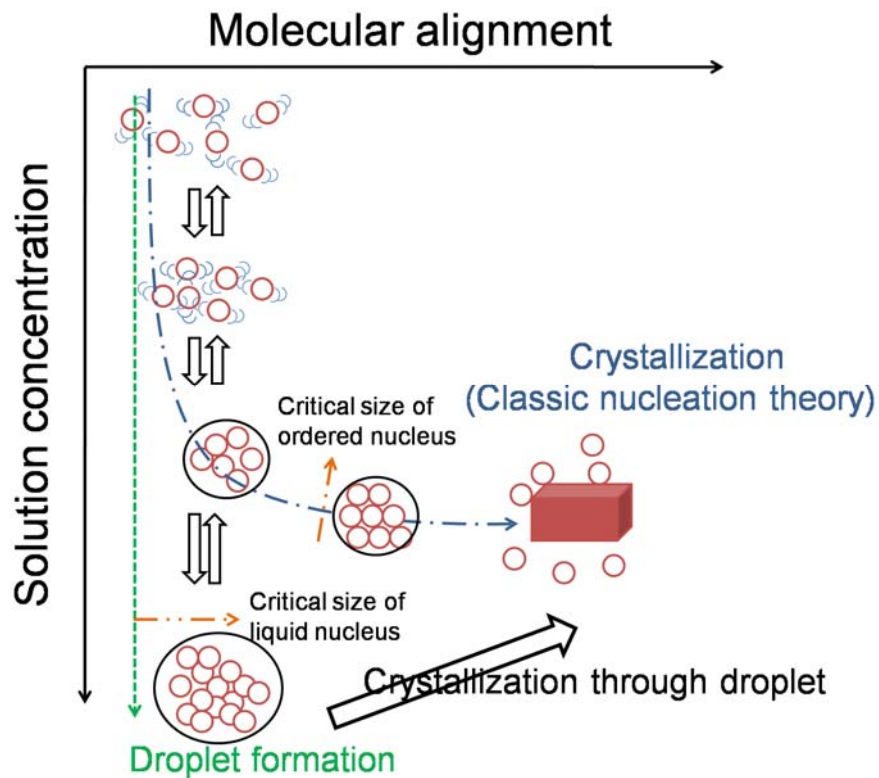
reasonably.

Fig. 6.6 Schematically illustrating the droplet formation and crystallization based on concentration and molecule alignment.
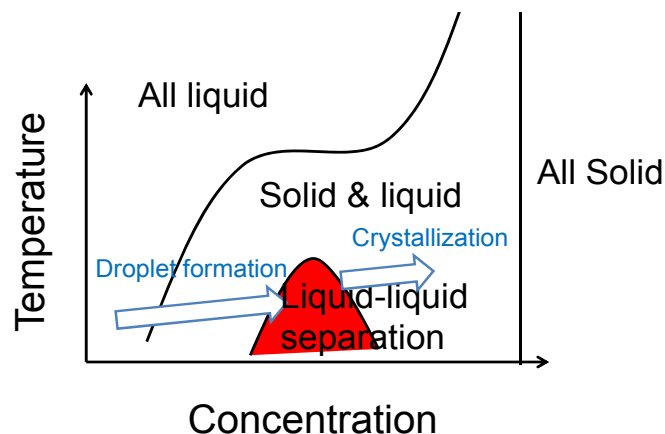
Fig. 6.7 Phase diagram showing temperature and concentration dependent phase transition. Arrow indicates transition path from liquid to liquid-liquid separation phase.

6.5 Droplet formation: Compared with different solvents

As mentioned above, dense liquid droplet is formed by cooperation of photon pressure and Marangoni effect. It has been reported that surface deformation is the indispensable process for droplet formation [2]. We found the solution deformation both in proline/D_2O and proline/EtOD but droplet formation was observed only latter.

To consider different droplet formation tendencies in D_2O and EtOD from energetic view points, a schematic free energy diagram is drawn as depicted in Fig. 6.8. Horizontal and vertical axes express stage of droplet formation and free energies of the droplet formation in proline/D_2O and proline/EtOD. Droplet formation is influenced on elemental phenomena such as photon pressure, surface deformation, temperature elevation and molecular interactions. We assume that the same initial free energy in two solutions.

The droplet formation can be considered as one kind of phase transition from view point of

molecular arrangement conversion. Solute-solute interaction will be strengthened during the droplet formation because too many molecules are packed in small space of droplet. It has reported that the effects of hydrogen bonding with a water molecule on the relative stability of the low energy conformers of proline [11]. On the other hand, the higher energy for droplet formation(less water) in proline/D_2O solution can be suggested. Oppositely, there is no big influence in EtOD solution on droplet formation so that relatively small energy difference between initial state and droplet formation is suggested.

Photon pressure which collects molecules at the focal spot is indispensable for droplet formation and increase energy to overcome energy barrier for droplet formation. Focused laser induced temperature elevation, and it caused surface deformation with thinning of solution layer which enhanced mass transfer due to thermal capillary.

On the other hand, temperature increase due to laser irradiation increases thermal disturbance and suppresses molecular trapping. Thermal interference for droplet formation in EtOD should be energetically much larger compare with that in D_2O. However we did not observe droplet in D_2O but in EtOD. It suggests other negative contribution to prevent droplet formation and it should be the strong molecular interaction between solute and solvent molecules. It has reported that strong hydrogen bonding between them so that photon pressure can not trap proline molecules easily to form droplet [12, 13]. Oppositely, it should be less influence in EtOD solution on droplet formation.
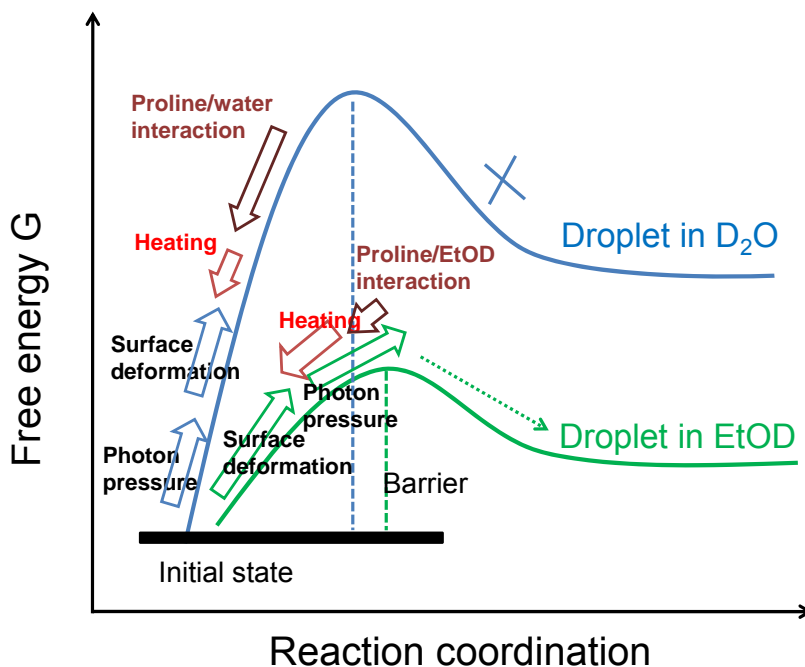
Fig. 6.8 Schematic drawing of free energy for droplet formation in different solvent

Combination of above mentioned positive and negative influences determine that it can overcome the barrier or not to form the dense droplet.
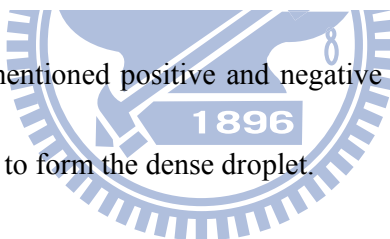
6.6 Summary

We proposed droplet formation dynamics based on experimental observation of its formation process. Droplet is formed by the cooperation of Managoni effect and photon pressure. Observed droplet formation of proline in EtOD is similar to that observed in glycine in D_2O. However, temperature elevation in EtOD should be higher than that in D_2O and it prevents effective droplet formation and crystallization in EtOD. For example, crystallization took place through the liquid droplet reflects high temperature elevation is

negative effect for crystallization. It increases the molecular motion so that slow droplet formation and growth. Beside, droplet is difficult to be observed under higher laser power in proline/EtOD because surface height decreasing is too quick to trap enough molecules for the droplet formation.

Irradiation induced obvious increase of backward scattering intensity increase reflects clearly concentration increase due to the laser trapping.

Droplet formation is considered as liquid-liquid separation. It is formed through rapid concentration increase in short time so that molecules cannot arrange well. A reason of droplet formation only in EtOD but not in D_2O can be explained in view point of high free energy of droplet formation in D_2O; strong interaction between water and proline molecules need high energy to brake interaction.
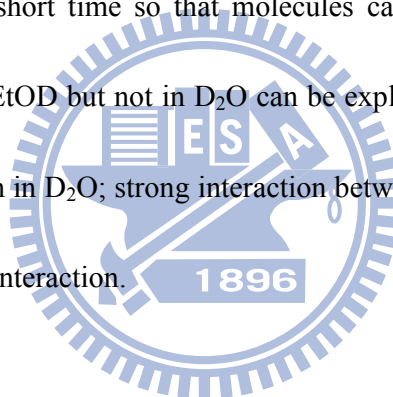
6.7 Reference

1. H. Masuhara, T. Sugiyama, T. Rungsimanon, K.-i. Yuyama, A. Miura, and J.-R. Tu, *Laser-trapping assembling dynamics of molecules and proteins at surface and interface.* Pure Appl. Chem., 2011. **83**: p. 869-833.

2. K.-i. Yuyama, K. Ishiguro, T. Rungsimanon, T. Sugiyama, and H. Masuhara, *Single droplet formation and crystal growth in urea solution induced by laser trapping.* Proc. of SPIE, 2010. **7762**.

3. K.-i. Yuyama, T. Sugiyama, and H. Masuhara, *Millimeter-Scale Dense Liquid Droplet Formation and Crystallization in Glycine Solution Induced by Photon Pressure.* J. Phys. Chem. Lett., 2010. **38**: p. 1321-1325.

4. G.D. Costa, *Optical visualization of the velocity distribution in a laser-induced thermocapillary liquid flow.* Applied Optics, 1993. **32**: p. 2144-2151.

5. G.D. Costa and J. Calatroni, *Transient deformation of liquid surfaces by laser-induced thermocapillarity.* Applied Optics, 1979. **18**: p. 233-235.

6. O.A. Louchev, S. Juodkazis, N. Murazawa, S. Wada, and H. Misawa, *Coupled laser molecular trapping,cluster assembly, and deposition fed by laser-induced Marangoni convection.* Optics Express, 2008. **16**: p. 5673-5680.

7. B.A. WRIGHT and P.A. COLE, *Preliminary examination of the crystal structure of l-proline.* Aeta Cryst., 1949. **2**: p. 129-130.

8. E. Romano , F. Suvire, M.E. Manzur, S. Wesler, R.D. Enriz, and M.A.A. Molina, *Dielectric properties of proline: Hydration effect.* Journal of Molecular Liquids, 2006. **126**: p. 43-47.

9. P.G. Vekilov, *Dense Liquid Precursor for the Nucleation of Ordered Solid Phases from Solution.* Crystal Growth & Design, 2004. **4**.

10. P.E. Bonnett, K.J. Carpenter, S. Dawsona, and R.J. Davey, *Solution crystallisation via a submerged liquid–liquid phase boundary:oiling out.* Chem. Commun, 2003: p. 689-699.

11. K.-M. Lee, S.-W. Park, I.-S. Jeon, B.-R. Lee, D.-S. Ahn, and S. Lee, *Computational Study of Proline-Water cluster.* Bull. Korean Chem. Soc., 2005. **26**: p. 909-912.

12. M. Civera, M. Sironi, and S.L. Fornili, *Unusual properties of aqueous solutions of L-proline:A molecular dynamics study.* Chemical Physics Letters, 2005. **415**: p. 274-278.

13. B. Schobert and H. Tschesche, *Unusual solution properties of proline and its interaction with proteins.* Biochimica et Biophysica Acta, 1978. **541**: p. 270-277.

7. Summary

In this study we examined laser trapping-induced crystallization of L-proline by focusing near-infrared laser to the air/solution interface of different solvents such as D_2O, EtOD and its mixture. We carried out microscopic observations of surface deformation, dense liquid droplet formation and crystallization processes in different solvents and discussed it dynamics and mechanism of observed trapping laser-induced crystallization and related phase transition phenomena.

In chapter 3, we examined laser trapping crystallization of proline in D_2O. Microscopic imaging of crystallization process with surface deformation dynamics observation revealed solution deformation and following crystallization or local dry spot formation. Poor crystallinity of formed flat polycrystal only within very thin solution layer and frequently observed local dry spot formation suggests that photon pressure works ineffectively for forming molecular assembly of proline in D_2O due to too strong solute-solvent interaction.

In chapter 4, we examined laser trapping crystallization of proline in mixed solvent of D_2O and EtOD. We succeeded inducing crystallization of proline in mixed solvent. It gives important suggestion that a photon pressure-induced crystallization possibility can be raised by adjusting solvent condition such as controlling of solubility and/or of interaction strength between solute and solvent molecules.

In chapter 5, we examined laser trapping crystallization of proline in EtOD and successfully demonstrated photon pressure induced crystallization for the first time although formed crystal disappeared by terminating the trapping laser light. Characterization of formed crystal done by polarization microscopy, SHG and Raman spectroscopy indicates formed crystal is proline crystal. We found that crystallization of proline frequently achieved through dense liquid droplet formation and we succeeded the observation of primal droplet formation process under microscope. It is also the first report of proline droplet formation in EtOD. Since previously reported droplet formation of several amino acids have done with larger scale such as sub-millimeter, microscopic observation of droplet formation and growth dynamics is one of the significant achievements in this study.

In chapter 6, we have discussed droplet formation dynamics and contribution for crystallization. Backward scattering spectroscopy at the focal spot during droplet formation experimentally indicates very local concentration elevation around focal spot of trapping laser and strongly indicates the formation of dense liquid droplet. Comparisons with the droplet of glycine in D_2O suggest similarity with that observed in proline/EtOD and suppose similar mechanism of crystallization through liquid-liquid phase separation.

As a result, we successfully demonstrated crystallization of proline by choosing different solvents. Attempts done in different solvents revealed that solvent dependent obvious assembling dynamics and crystallization process change. It suggests that crystallization

induced by laser trapping is trigged by local molecular assembling of solute molecules

which exist in quite different environment depending on surrounding solvent molecule and

such molecular environment difference critically affects to crystallization. Results obtained

in this study not only greatly contributed for understanding of laser trapping crystallization

dynamics and mechanism but also clearly demonstrated a novel photoscience of photon

pressure utilized molecular assembly formation.